Tumors of Connective Tissue

13

A. M. De Schepper, J. E. Vandevenne

Contents

13.1 Introduction

Fibrous tissue consists of fibroblasts and an extracellular matrix containing both fibrillary structures (collagen, elastin) and nonfibrillary, gel-like ground substance. Both fibroblasts (spindle-shaped cells) and myofibroblasts, which are modified fibroblasts showing features common to fibroblasts and smooth muscle cells, produce procollagen and collagen. Collagen is the main, noncontractile component of the extracellular matrix, elastin is the main, contractile component of elastic fibers. The amorphous ground substance of fibrous tissue contains glycosaminoglycans (mucopolysaccharides), the most common types being hyaluronic acid, chondroitin 4- and 6-sulfates, and proteoglycans. [56] Fibrous tissue can be loose or dense depending on the relative amount of the three components. Dense fibrous tissue is seen in tendons, ligaments, and aponeuroses.

Fibroblastic/myofibroblastic tumors represent a very large subset of mesenchymal tumors. Many lesions in this category contain cells with both fibroblastic and myofibroblastic features, which may in fact represent functional variants of a single cell type. The relative proportions of these cell types vary not only between individual cases but also within a single lesion over time (often in proportion to cellularity). A significant subset of spindle cell and pleomorphic sarcomas are probably myofibroblastic in type, but, to date, only low-grade forms have been reproducibly characterized. Among lesions formerly known as malignant fibrous histiocytoma (MFH), at least some represent pleomorphic myofibrosarcomas.

Principal changes and advances since the 1994 WHO classification have been the characterization of numerous previously undefined lesions, including ischemic fasciitis, desmoplastic fibroblastoma, mammary-type myofibroblastoma, angiomyofibroblastoma, cellular angiofibroma, Gardner fibroma, low-grade fibromyxoid sarcoma, acral myxoinflammatory fibroblastic sarcoma, sclerosing epithelioid fibrosarcoma, and low-grade myofibroblastic sarcoma.

Conceptual changes have included the clearer recognition of solitary fibrous tumor in soft tissue and the realization that most cases of so-called hemangiopericytoma belong in this category, as well as the reclassification of lesions formerly labeled "myxoid MFH" as "myxofibrosarcoma" and the definitive allocation of the tumors to the fibroblastic category.

The new (2002) WHO classification of fibroblastic/myofibroblastic tumors [20] contains a large number of

new and modified lesions. They are categorized into four groups according to their degree of malignancy, i.e., (1) benign, (2) intermediate (locally aggressive), (3) intermediate (rarely metastasizing), and (4) malignant:

1. **Benign:**
   - Nodular fasciitis
   - Proliferative fasciitis
   - Proliferative myositis
   - Myositis ossificans
   - Fibro-osseous pseudotumor of digits
   - Ischemic fasciitis
   - Elastofibroma
   - Fibrous hamartoma of infancy
   - Myofibroma/Myofibromatosis
   - Fibromatosis colli
   - Juvenile hyaline fibromatosis
   - Inclusion-body fibromatosis
   - Fibroma of tendon sheath
   - Desmoplastic fibroblastoma
   - Mammary-type myofibroblastoma
   - Calcifying aponeurotic fibroma
   - Angiomyofibroblastoma
   - Cellular angiofibroma
   - Nuchal-type fibroma
   - Gardner fibroma
   - Calcifying fibrous tumor
   - Giant cell angiofibroma
2. **Intermediate (locally aggressive):**
   - Superficial fibromatoses (palmar/plantar)
   - Desmoid-type fibromatoses
   - Lipofibromatosis
3. **Intermediate (rarely metastasizing):**
   - Solitary fibrous tumor and hemangiopericytoma (including lipomatous hemangiopericytoma)
   - Inflammatory myofibroblastic tumor
   - Low-grade myofibroblastic sarcoma
   - Myxoinflammatory fibroblastic sarcoma
   - Infantile fibrosarcoma
4. **Malignant:**
   - Adult fibrosarcoma
   - Myxofibrosarcoma
   - Low-grade fibromyxoid sarcoma hyalinizing spindle-cell tumor
   - Sclerosing epithelioid fibrosarcoma

In the case of several fibroblastic proliferations (elastofibroma, fibroma of tendon sheath, extra-abdominal desmoids, fibromatosis colli), it is unclear whether these constitute reactive fibrosing processes or true neoplasms. Fibromatoses are aggressive, infiltrating lesions, despite their histologically benign character, and aggressive fibromatoses or musculoaponeurotic desmoid tumors are by far the largest group of tumors of fibrous tissue. The terminology of childhood fibromatosis is confusing, and there are many classification systems based on different clinicopathological parameters such as age, localization, histology, and aggressiveness of the lesion [86]. Fibrous tumors of infancy and childhood and soft tissue fibrosarcomas are rare and have only sparsely been reported in the radiological literature. It is a constant finding that the majority of these tumors have a high recurrence rate after surgical resection, and recurrent lesions mostly have a more aggressive behavior than their primary counterparts. Another constant finding is the natural evolution of tumors of fibrous tissue, which are hypercellular in their initial stage and become more collagenous in later stages. Localization of the lesion and age of the patient are major diagnostic factors. Fibroma of tendon sheath, elastofibroma, all types of fibromatosis, and fibromatosis colli are characterized by typical localizations [30, 85].

13.2 Benign Fibroblastic Proliferations

Benign fibroblastic proliferations constitute a heterogeneous group of well-defined entities. Some of these, such as nodular fasciitis, grow rapidly and are richly cellular. Others, such as fibroma of the tendon sheath and elastofibroma, grow slowly, are much less cellular, and contain considerable amounts of collagen [17, 71].

13.2.1 Nodular Fasciitis

Nodular fasciitis, also called pseudosarcomatous fasciitis, infiltrative fasciitis, or proliferative fasciitis, is a benign soft tissue lesion composed of proliferating fibroblastic-myofibroblastic cells. It is characterized by rapid growth, which may arouse suspicion of sarcoma [47]. Although the cause is unknown, it is likely that it is triggered by local injury or a local inflammatory process. Most patients are asymptomatic or note only mild discomfort. Lesions are round to oval and mostly located in the upper extremity (48%), mostly the volar aspect of the forearm [83], trunk (20%), head and neck (17%), and lower extremity (5%) [42, 59]. Shimizu has reported on a series of 250 patients with a mean age of 39 years and a peak in the fourth decade, in whom 44% of the lesions are located in the upper extremity, which is followed in frequency by the lower extremity and the trunk [75]. Although no sex predilection for nodular fasciitis is mentioned in literature, we reported on a series of ten patients, nine of them being female [83]!

There are three subtypes of nodular fasciitis, defined according to their topography: the most common subcutaneous type, the intramuscular type, and the fascial type, which spreads along superficial fascial planes. Microscopically, younger lesions consist of fibroblasts embedded in a dense reticulin meshwork and birefringent collagen. There is a rich intervening myxoid matrix. Older lesions tend to be more fibrous. In this re-

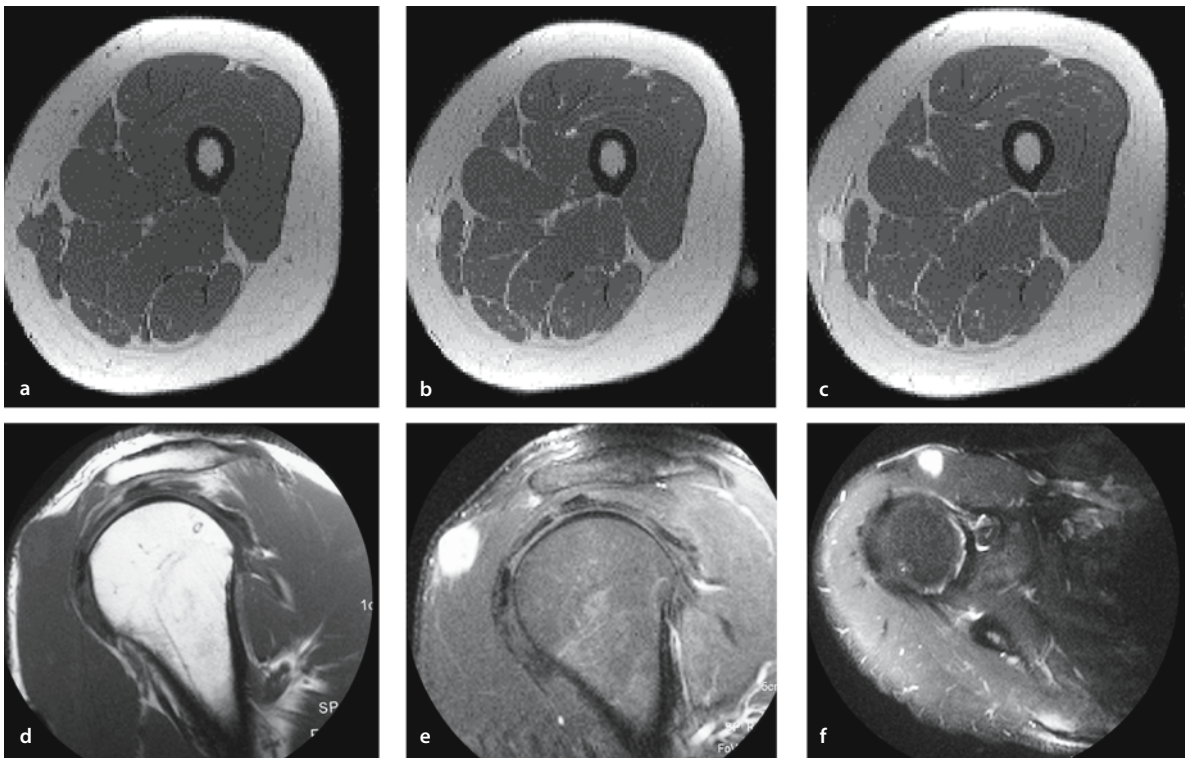

Fig. 13.1 a–f. Two cases of nodular fasciitis, fascial type: a first case (**a–c**) at the fascia of the sartorius muscle, a second case (**d–f**) at the fascia of pectoralis muscle. **a** Axial spin-echo T1-weighted MR image. **b** Axial spin-echo T1-weighted MR image after gadolinium contrast injection. **c** Axial spin-echo T2-weighted MR image. **d** Sagittal spin-echo T1-weighted MR image. **e** Sagittal spin-echo T1-weighted MR image after gadolinium contrast injection, with fat suppression. **f** Axial spin-echo T2-weighted MR image. Both lesions are in close contact with superficial fasciae. On T1-weighted images, both lesions are of slightly higher signal intensity (SI) when compared with SI of normal muscle (**a**, **d**). They both enhance markedly after contrast injection (**b**, **e**) and are of high SI on T2-weighted MR images (**c**, **f**)

gard, nodular fasciitis can be subdivided into three types based on the predominant histological features: myxoid (type 1), cellular (type 2), and fibrous (type 3). However, since many different features may coexist in one lesion, definition of a single fixed type is not always possible. There is no correlation between histological subtypes and the subtypes classified according to their anatomical location. Histological transformation from type 1 to type 2 and then to type 3 is indicative of the natural evolution of these lesions. Recurrence after excision is very rare and occurs in less than 2% of the cases.

On ultrasound images, lesions of this kind are mostly solid, and cystic change has been reported (Fig. 13.2a). On CT scans, nodular fasciitis has low attenuation values, reflecting the myxoid character of the lesions [59]. The appearance on MR images reflects the gross morphology of the tumor. Myxoid and cellular lesions are iso- to hyperintense compared with skeletal muscle on T1-weighted images and iso- to hyperintense compared with fat on T2-weighted images. Lesions with a more fibrous histology are markedly hypointense on all spin-echo sequences [59]. Myxoid lesions show a marked and homogeneous enhancement, cellular lesions a nonhomogeneous enhancement, and fibrous lesions a moderate, nonhomogeneous enhancement [83]. Three cases in our own series had the same appearance on MR images: a central area of low signal intensity (SI) and a peripheral area of higher SI on T1-weighted images, and an inverted SI pattern (high SI of the center, and low SI of the periphery) on T2-weighted images. After gadolinium (Gd) contrast injection there is a marked enhancement of the peripheral zone, with poor enhancement of the center. This pattern was described in 1991 by Frei et al. [25]. On comparing these findings with the MR features of some neurogenic tumors (target sign), we named the pattern "the inverted target sign" (Figs. 13.1, 13.2).

The cellular type of nodular fasciitis is apt to be mistaken for a sarcoma (myxofibrosarcoma and fibrosarcoma), while the fibrous type must be differentiated from fibromatosis. Recurrent tumors have a more aggressive behavior than primary ones (Fig. 13.3).

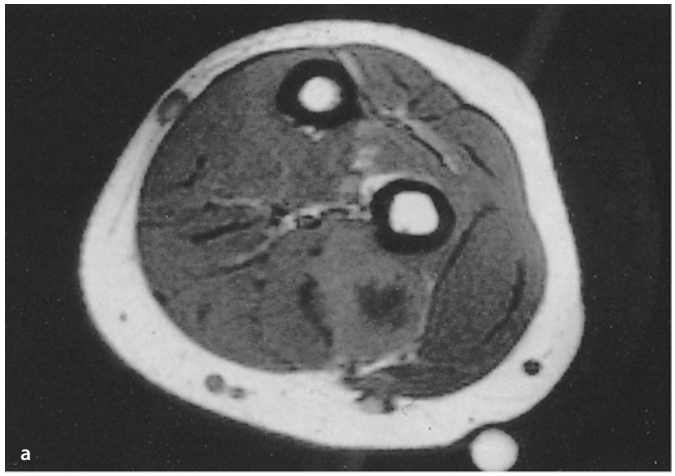
a

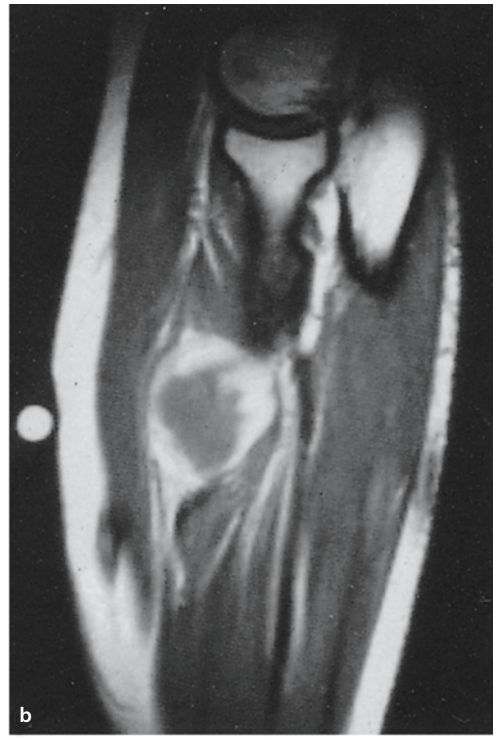
b

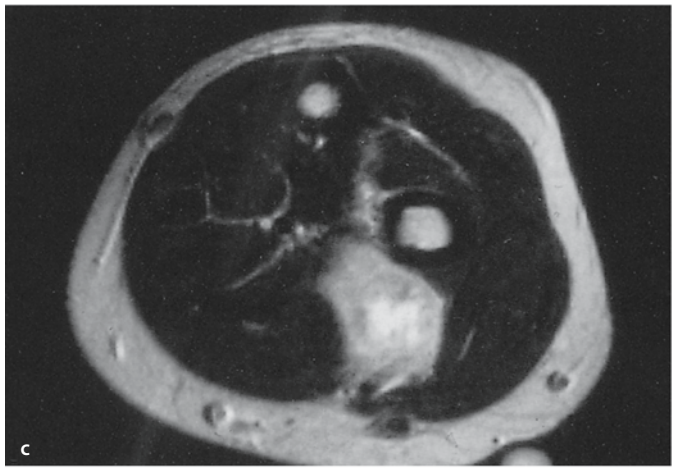
c

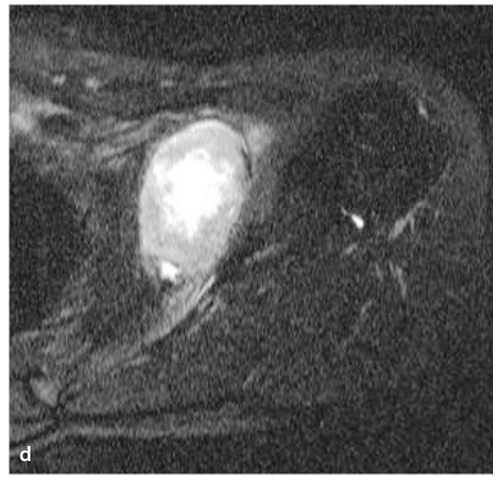
d

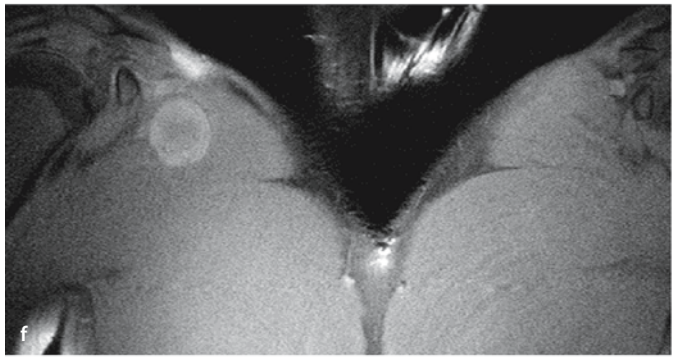
f

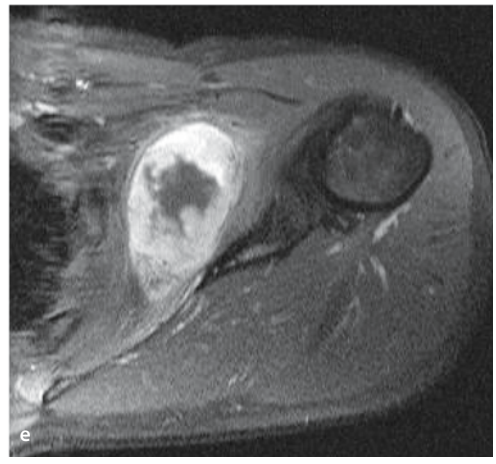
e

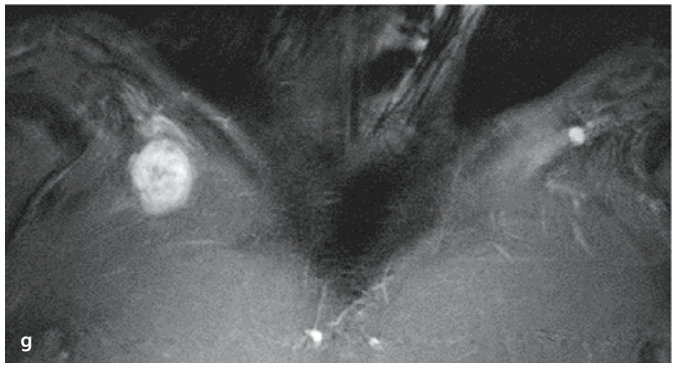
g

Fig. 13.2 a–g. Three cases of nodular fasciitis, intramuscular type: the first case (**a–c**) at the forearm, the second case (**d**, **e**) at the subscapularis muscle, and the third case (**f, g**) at the pectoralis muscle. **a** Axial spin-echo T1-weighted MR image. **b** Coronal spin-echo T1-weighted MR image after gadolinium contrast injection. **c** Axial spin-echo T2-weighted MR image. **d** Axial spin-echo T2-weighted MR image. **e** Axial spin-echo T1-weighted MR image after gadolinium contrast injection, with fat suppression. **f** Coronal spin-echo T1-weighted MR image, with fat suppression. **g** Coronal spin-echo T1-weighted MR image after gadolinium contrast injection, with fat suppression. All three cases present with the so called "inverted target" sign consisting of a peripheral zone of increased SI on T1-weighted MR images (**a**, **f**), decreased SI on T2-weighted MR images (**c**, **d**) and merely peripheral contrast enhancement (**b**, **e**, **g**)

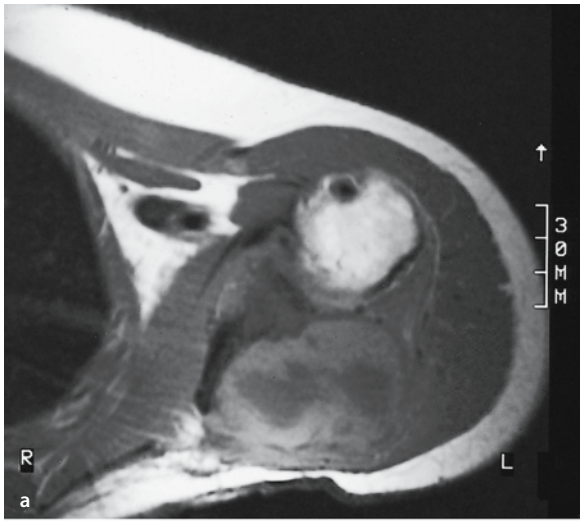

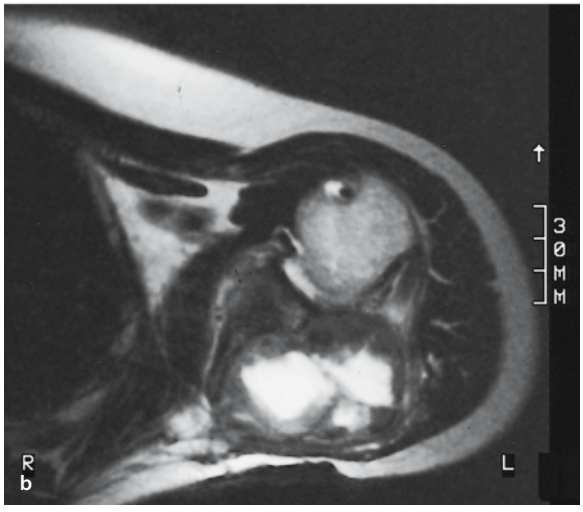

Fig. 13.3 a, b. Recurrent nodular fasciitis of the fascial type in a 37-year-old woman. **a** Axial spin-echo T1-weighted MR image. **b** Axial spin-echo T2-weighted MR image. Well-delineated, oval mass within the region of the infraspinatus muscle, adjacent to the scapula. The lesion is hyperintense to muscle on the T1-weighted image, with a central, bilobate area of lower signal intensity (**a**). Central parts of the lesion show high signal intensity on the T2-weighted image (**b**), while the peripheral component remains of lower signal intensity. This case also illustrates the "inverted target sign"

13.2.2 Fibroma of Tendon Sheath

Fibroma of the tendon sheath consists of a benign, slow-growing, dense fibrous nodule (or multinodular mass) firmly attached to the tendon sheath and is found most frequently in the hands and feet (Fig. 13.4). The thumb, index finger, and middle finger together with lesions of

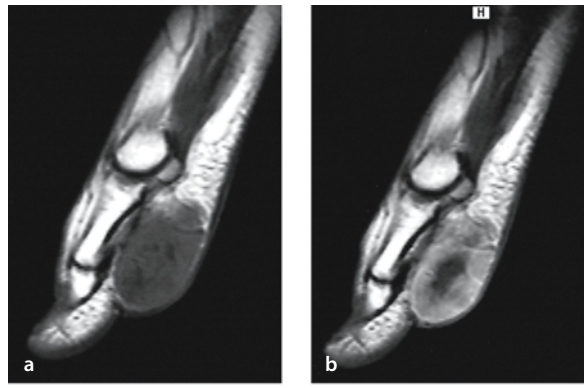

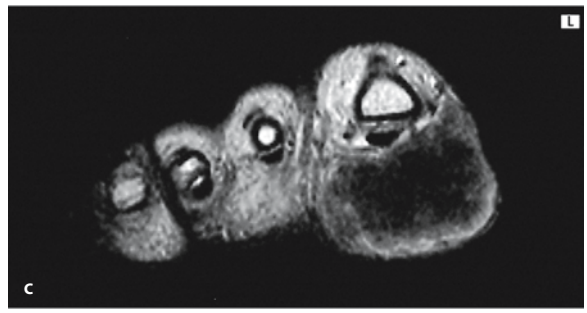

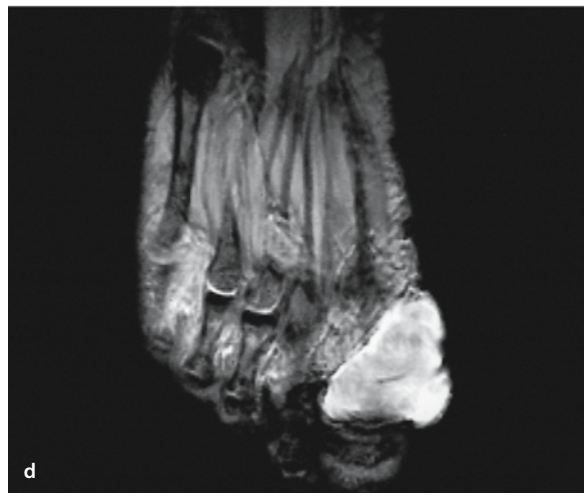

Fig. 13.4 a–d. Fibroma of tendon sheath in a 35-year-old woman. **a** Sagittal spin-echo T1-weighted MR image. **b** Sagittal spin-echo T1-weighted MR image after gadolinium contrast injection. **c** Axial spin-echo T2-weighted MR image. **d** Coronal gradient T2*-weighted image. Large, oval mass at the plantar aspect of the left great toe. The lesion is inhomogeneous and ill-defined at the proximal pole (**a**). After contrast injection there is marked enhancement at the periphery of the lesion (**b**). On the T2-weighted image, the whole lesion is of low signal intensity (**c**). On gradient-echo sequence, the periphery of the lesion is of extremely high signal intensity (**d**)

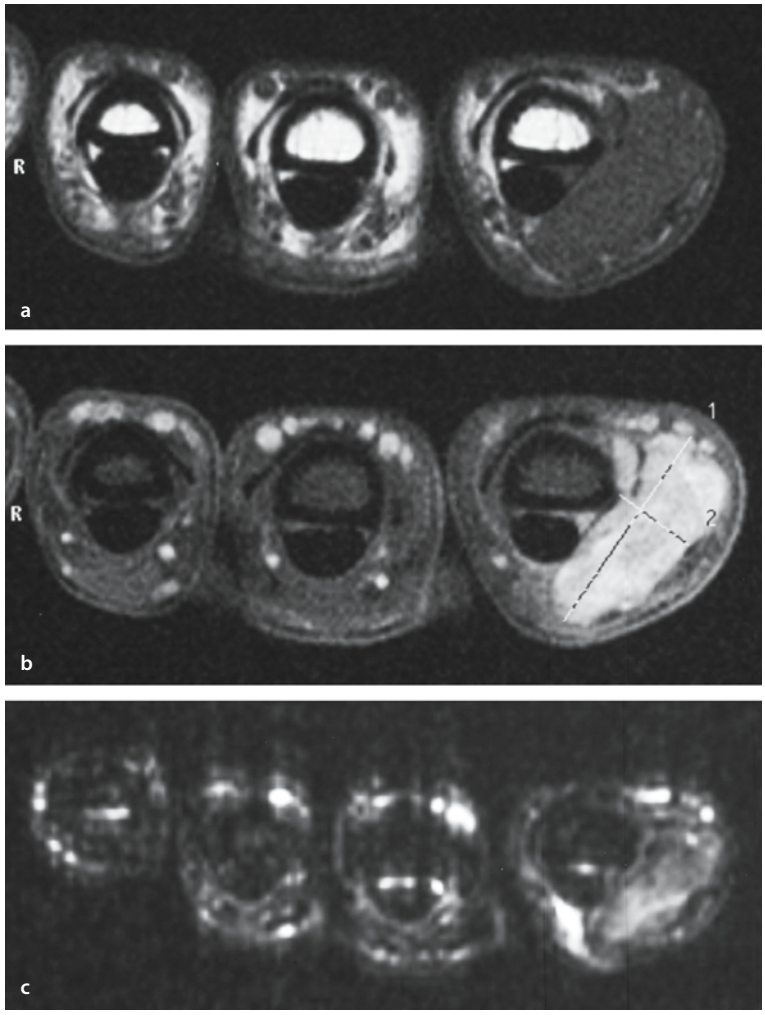

Fig. 13.5 a–c. Fibroma of tendon sheath at the volar aspect of the third finger adjacent to the flexor tendon. **a** Axial spin-echo T1-weighted MR image. **b** Axial spin-echo T1-weighted MR image after gadolinium contrast injection with fat suppression. **c** Axial spin-echo T2-weighted MR image with fat suppression. The lesion is of low SI on T2-weighted MR images (**c**) and enhances moderately after gadolinium contrast injection (**b**)

the volar aspect of the wrist account for 80 % of cases. It is considered to be either a reactive fibrosing process or a benign neoplasm. It is found most commonly in adults and is more than twice as common in men as in women. The main symptom is a small mass that rarely measures more than 2 cm and is painless but may limit motion of the involved digit [52]. Macroscopically, it resembles the lobular configuration of the much more common giant cell tumor of the tendon sheath, but it is less cellular and there are no xanthoma cells or giant cells [17]. Microscopically this lobulated nodular lesion is composed of tightly packed spindle cells (fibroblasts), vessels, and large amounts of dense collagenous material, which is markedly hyalinized. Occasionally there is a gradual transition from the poorly cellular hyalinized collagenous areas to more cellular areas which are thought to be characteristic of the early stages of the tumor development. More cellular forms must be differentiated from nodular fasciitis, fibrous histiocytoma, and even fibrosarcoma.

Although fibromas of the tendon sheath may resemble nodular fasciitis histologically, they involve hands and feet almost exclusively and are slow-growing lesions, while lesions of nodular fasciitis appear suddenly, grow rapidly, and usually attain full size in 3–6 weeks. Moreover, they have a predilection for the volar aspect of the forearm [67].

Plain radiographic findings in a fibroma of tendon sheath eroding the third metatarsal have been reported by Lourie et al. [52].

Fox et al. [23] have reported on a series of six patients with fibroma of the tendon sheath. Findings from MRI were not at all specific, i. e., low to intermediate SI on both T1- and T2-weighted images and a variable enhancement (from none to markedly enhanced) after contrast administration. MR findings depend on and reflect the relative amount of different tumor components that are cellular, myxoid, vascular, or collagenous. As a consequence there can be overlap in MR findings with features of giant cell tumor of the tendon sheath (Fig. 13.5).

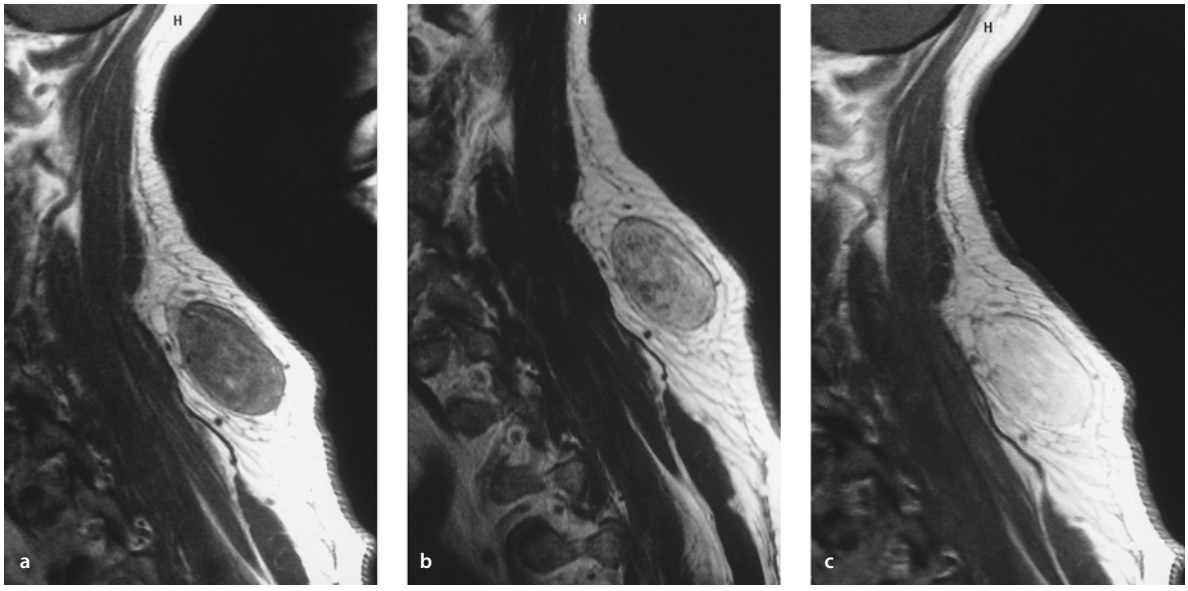

Fig. 13.6 a–c. Nuchal fibroma in a 50-year-old man. **a** Sagittal spin-echo T1-weighted MR image. **b** Sagittal spin-echo T2-weighted MR image. **c** Sagittal spin-echo T1-weighted MR image after gadolinium contrast injection. Oval, well-delineated mass within the subcutaneous fatty tissue of the neck. There is an intermediate signal intensity on both spin-echo images owing to the mixed histological composition of entrapped fat within a collagenous mass (**a**, **b**). There is marked enhancement after contrast injection (**c**). Localization and MR presentation are characteristic of a nuchal fibroma

13.2.3 Nuchal Fibroma

Nuchal fibroma, or collagenosis nuchae, is a benign soft tissue tumor that arises from the posterior cervical subcutaneous tissue, with a predilection for the interscapular and paraspinal regions. Nuchal fibroma is significantly more common in men, with a peak incidence during the third to the fifth decades.

Microscopically, nuchal fibromas have a superficial (subcutaneous or dermal) component and consist of paucicellular, thick bundles of lobulated collagen fibers with inconspicuous fibroblasts. Entrapped adipose tissue and traumatic neuroma-like nerve proliferations are typically present. Skeletal muscle infiltration is also seen in a minority of cases. The process has a strong association with diabetes and also appears to be linked to Gardner's syndrome, fibromatosis, and dermatofibrosarcoma protuberans. Local recurrence probably reflects the persistence of local or systemic factors related to its pathogenesis [60, 72].

The MR appearance reflects the histological composition: collagen has a low SI both on T1- and T2-weighted images. Small foci of high SI on T1-weighted images are due to entrapped adipose tissue (Figs. 13.6, 13.7). In this regard there is a strong similarity to elastofibromas.

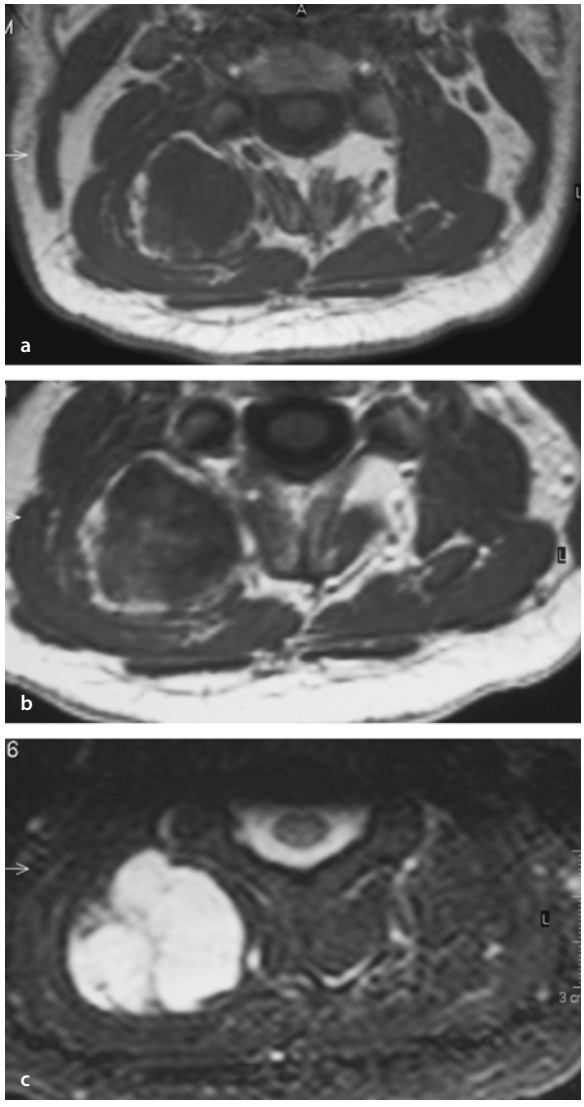

Fig. 13.7 a–c. Nuchal fibroma. **a** Axial spin-echo T1-weighted MR image. **b** Axial spin-echo T1-weighted MR image after gadolinium contrast injection. **c** Axial short-tau inversion recovery (STIR) MR image. Atypical presentation of a nuchal fibroma with high SI on STIR sequence (**c**) and minimal, cloudy enhancement after contrast injection (**b**)

13.2.4 Elastofibroma

Elastofibroma is generally considered to be a fibroelastic pseudotumor. It occurs almost exclusively in the subscapular region beneath the rhomboideus major and latissimus dorsi muscles adjacent to the inferior angle of the scapula. It is thought to be caused by repeated mechanical friction between the chest wall and the tip of the scapula, which was the site of the lesion in 99% of the reported cases. Other locations, albeit uncommon, include the infraolecranon, thoracic wall, axilla, and greater trochanter regions. Bilateral lesions are common and seen in 10–60% of patients. Most patients are older adults, and there is a definite predominance in women. Single cases have been reported in children [12]. Half of the patients are asymptomatic, and 50% have pain on arm motion. Chromosomal abnormalities and familial occurrences support a genetic predisposition to elastofibroma dorsi.

On gross examination, these lesions are firm and rubbery [12, 47, 50, 55]. Histologically, lesions are composed mainly of elastin-like fibers and entrapped islands of mature adipose tissue. Microscopic examination shows hypertrophy and degeneration of elastin with a background of mature collagen and fat. CT scans show attenuation similar to that of adjacent muscle. Sometimes there are strands of low density similar to that of subcutaneous fat [48] (Fig. 13.8a). MRI nicely reflects the histological composition of entrapped fat within a predominantly fibrous mass. On both T1- and T2-weighted images, the lesion presents as a lenticular, well-defined mass with an intermediate SI approximately equal to that of skeletal muscle. Interlaced areas have a SI similar to that of fat [45]. Areas of low SI on both T1- and T2-weighted images correspond histologically to fibroelastic tissue [48] (Fig. 13.8b–d).

Surgery should not be performed for diagnostic purposes in elderly individuals. Indeed, familiarity of the radiologist with this entity may make it possible to avoid some surgery [54]. Differential diagnosis is limited, but includes older desmoids, which are hypocellular, contain large amounts of collagen, and occur in younger patients.

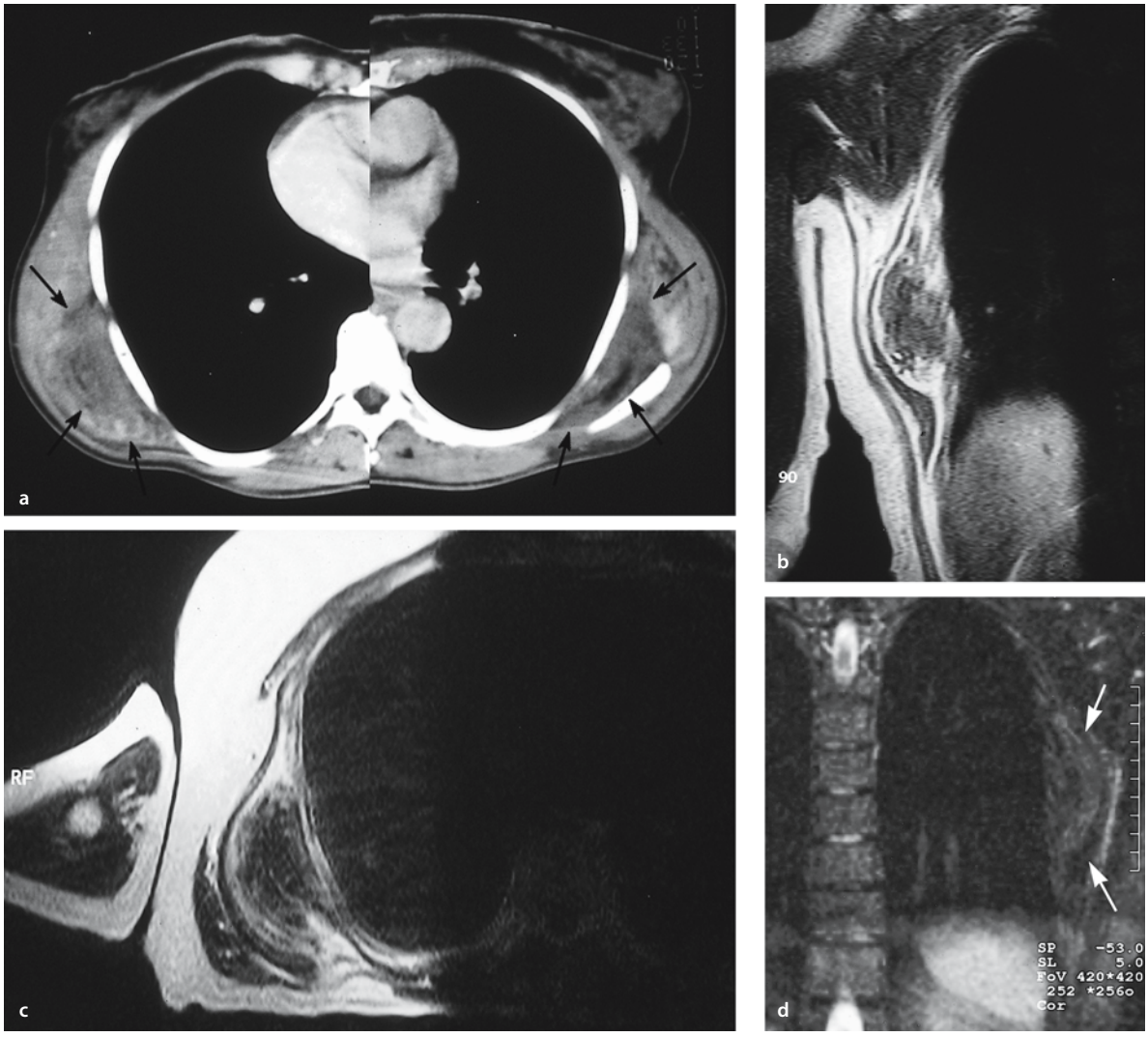

Fig. 13.8 a–d. Elastofibroma dorsi in a 60-year-old woman (**a**), in a 67-year-old woman (**b**, **c**), and in a 56-year-old woman (**d**). **a** CT scan after iodinated contrast injection. **b** Coronal spin-echo T1-weighted MR image. **c** Axial turbo spin-echo T2-weighted MR image. **d** Coronal STIR MR image. On the CT scan there is an oval mass between the rhomboid major and latissimus dorsi muscles on both sides (*arrows*). The lesions show mixed attenuation and enhancement after iodinated contrast injection (**a**). Oval mass within the subscapular region, showing signal intensity equal to that of fat and muscle on a T1-weighted image (**b**), and an overall low signal intensity on T2-weighted an on STIR images (**c**, **d**). Three cases of elastofibroma showing characteristic location, attenuation on CT scan, and signal intensity on MR images, reflecting the histological composition of entrapped fat within a fibrous mass

13.3 Fibromatoses

Fibromatoses cover a wide range of benign fibroblastic proliferations. They are classified according to Enzinger and Weiss into superficial and deep types, and are further subdivided according to anatomical location:

1. Superficial (fascial) fibromatosis
   a) Palmar fibromatosis (Dupuytren contracture)
   b) Plantar fibromatosis (Ledderhose disease)
   c) Penile fibromatosis (Peyronie disease)
   d) Knuckle pads
2. Deep (musculoaponeurotic) fibromatosis
   a) Extra-abdominal fibromatosis
   b) Abdominal fibromatosis
   c) Intra-abdominal fibromatosis:
      – Pelvic fibromatosis
      – Mesenteric fibromatosis
      – Gardner syndrome

Although both superficial and deep lesions have a similar microscopic appearance, superficial lesions are slow growing, while deep ones have a more aggressive biological behavior, between that of fibrosarcomas and fibromas [7]. Division into abdominal and extra-abdominal desmoids is arbitrary, since the lesions are histologically alike [5].

Fibromatoses are uncommon lesions, constituting 0.03% of all neoplasms. They are found in young adults, with a peak incidence at 30 years. There is no sex predominance, and most lesions are solitary, although synchronous multicentric lesions have been reported. A familial tendency has been observed. Local recurrence after surgery is seen in as many as 50% of patients [45].

Key criteria that establish the diagnosis are growth pattern, relationship with surrounding tissues, and cytological features. Lesions consist of uniform fibroblasts proliferating in a parallel way and intermingled with variable amounts of collagen. No atypical or hyperchromatic nuclei are found, while mitoses are infrequent. Generally, the most cellular areas are present in the center of the lesion, whereas the periphery has less numerous fibroblasts and greater amounts of dense collagen [24]. Although fibromatoses are histologically benign, their relationship to adjacent tissue is marked by interdigitating and infiltrative growth. Penile fibromatosis and intra-abdominal fibromatosis will not be discussed, since these do not belong to the locomotor system [68].

On ultrasound scans, fibromatoses appear as masses with low, medium, or high echogenicity and smooth, sharply defined borders. On CT images, the masses are either ill-defined or well circumscribed. Before contrast administration, desmoids show variable attenuation. After contrast administration, lesions usually have a higher attenuation than that of adjacent muscle [5].

In an attempt to explain the variable CT appearance of these lesions, Francis et al. have carried out a retrospective analysis of CT findings and histopathological features in nine patients with fibromatosis. In three of four patients who had precontrast CT scans, the tumors were hyperdense relative to muscle, while in one patient the lesion was hypodense. The postenhancement appearance was variable. The pathological specimens have been analyzed and graded for collagen content, cellular content, tumor necrosis, and tumor vascularity. No consistent relationship can be established between the CT appearance of these lesions and their histological appearance [24].

On MR images, most lesions demonstrate slightly increased SI relative to skeletal muscle on T1-weighted images and intermediate SI on T2-weighted images. The slight increase in SI on T1-weighted images is much less than that seen in lipomas and subacute hemorrhages. Enhancement pattern after contrast administration is variable.

Increased SI on T2-weighted images is seen in hypercellular lesions. Lesions that are hypointense or contain hypointense foci (linear or curvilinear) on both spin-echo sequences are found to be relatively hypocellular with abundant collagen. As a consequence, most lesions are rather inhomogeneous. Although usually well demarcated on MR images, microscopically fibromatosis is seen to invade adjacent structures [68].

The conditions that deserve consideration in the differential diagnosis of intra- and extra-abdominal desmoids are malignant lesions such as fibrosarcoma, rhabdomyosarcoma, synoviosarcoma, liposarcoma, myxofibrosarcoma, lymphoma, and metastases, and benign lesions such as neurofibroma, neuroma and leiomyoma, and acute hematoma of the rectus sheath and chest wall [5].

13.3.1 Palmar Fibromatosis

Palmar fibromatosis or Dupuytren contracture primarily involves palmar aponeurosis of the hand and its extensions. Usually the disease is diagnosed clinically on the basis of characteristic history and physical examination. The earliest clinical manifestation is the appearance of a subcutaneous nodule in the palm of the hand. As the disorder progresses, the overlying skin thickens and retracts, and a cord forms, producing progressive flexion contracture of the affected ray (Figs. 13.9, 13.10).

Palmar fibromatosis tends to affect adults, with a rapid increase in incidence with advancing age. It is bilateral in 40–60% of cases. The condition is by far more frequent in men and is most common in Northern Europe. Pathogenesis in both palmar and plantar

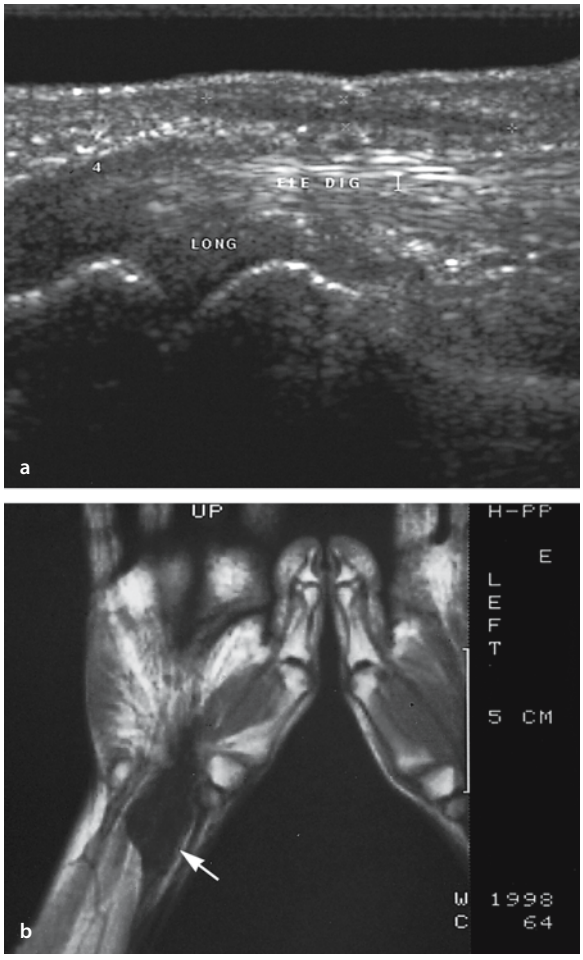

Fig. 13.9 a, b. Palmar fibromatosis in a 40-year-old man (ultrasound) (**a**) and in a 39-year-old woman (coronal spin-echo T1-weighted MR images) (**b**). In the first patient, the ultrasound image shows a cord- or plate-like hypoechoic lesion subcutaneously at the palmar aspect of the fourth metacarpophalangeal joint (**a**). In the second patient, there is a plate-like mass of low signal intensity within the carpal tunnel on the T1-weighted image (*arrow*; the lesion also had a low signal intensity on T2-weighted images, not shown) (**b**). Hypocellular type of cord- or plate-like palmar fibromatosis with characteristic location and imaging features on ultrasound and MR images

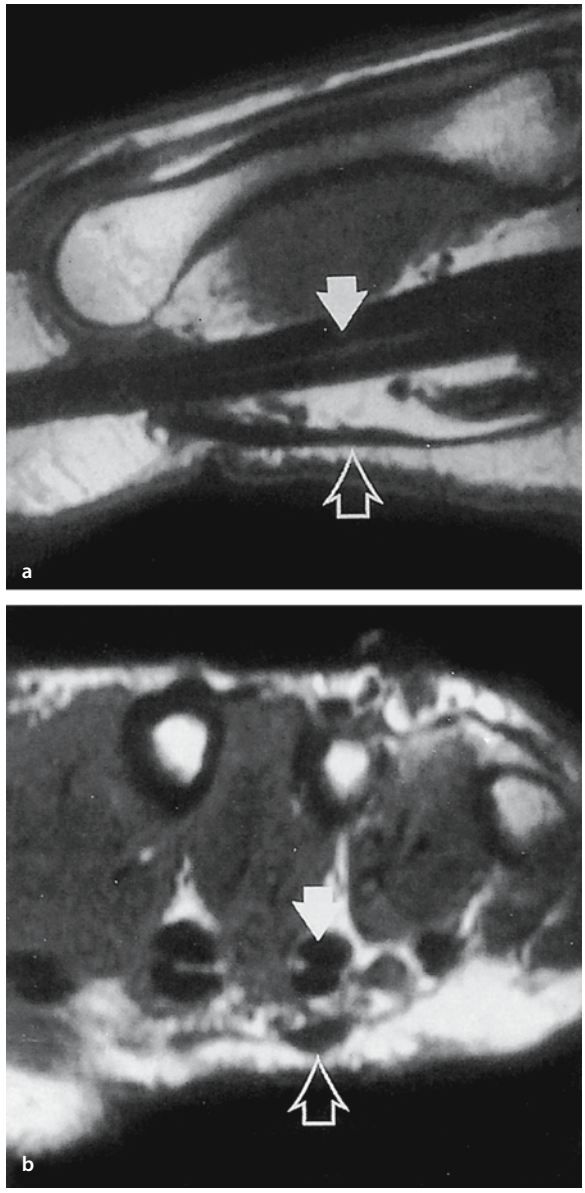

Fig. 13.10 a, b. Dupuytren contracture in a patient with palmar fibromatosis. **a** Sagittal spin-echo T1-weighted MR image. **b** Axial spin-echo T2-weighted MR image. There is a low signal intensity cord (*open arrows*) in the superficial palmar soft tissue at the level of the fourth metacarpal on the T1-weighted image (**a**) and a low signal intensity area superficial to the flexor tendon of the fourth ray (*white arrows*) on the T2-weighted image (**b**). This case illustrates the characteristic appearance of cord in Dupuytren contracture with signal intensity reflecting the hypocellular collagenous composition. (Reproduced from [87], with permission)

fibromatosis includes a genetic component, with family history and chromosome aberrations in 50% of cases.

Histologically, the nodules are quite cellular, composed of whorls of proliferative myofibroblasts. Cords contain a large amount of collagen and are hypocellular. The condition is treated surgically, but the recurrence rate is high (30–40%). The recurrence rate of lesions with mitotically active, cellular nodules is far higher (70%) than that of hypocellular lesions.

The appearance of the nodules and cords on MR images and the correlation between the SI and the lesion's degree of cellularity has been described by Yacoe et al. [87]. On MR images, the cords have a uniformly low SI (similar to the SI of tendon) on both T1- and T2-weighted images. In 18% of patients, nodules have a low to intermediate SI on T1-weighted images (slightly higher than that of tendon) and a low SI on T2-weighted images. Most nodules have an intermediate SI (similar to that of muscle) on both T1- and T2-weighted images. Only three nodules have a low SI on both T1- and T2-weighted images and were hypocellular on histological examination.

Signal characteristics of the lesions correlate with the degree of cellularity. The preoperative assessment of cellularity may be of prognostic significance, because highly cellular lesions tend to have a higher rate of recurrence after surgery than hypocellular lesions. As a consequence surgery may be delayed until the lesion matures and becomes more hypocellular and collagenous [23].

13.3.2 Plantar Fibromatosis

Plantar fibromatosis, also called Ledderhose disease, is a benign, fibroblastic, proliferative, and locally invasive disorder characterized by the replacement of elements of the plantar aponeurosis by abnormal fibrous tissue, which slowly invades the skin and the deep structures (Fig. 13.11)

The plantar aponeurosis is a strong band which originates at the inner tubercle of the calcaneus and contains two layers: a superficial layer which extends to the four smaller toes and a deeper layer which runs from lateral to medial and appears as a separate band to the great toe [49]. On ultrasound scans, the plantar aponeurosis is noted as a bright linear interface, approximately 5–8 mm from the surface of the sole [69]. On MR images the aponeurosis is seen as a thin linear strip of low SI that originates at the inferior border of the calcaneus and inserts into the distal flexor tendons near the metatarsophalangeal joints.

The etiology of plantar fibromatosis is unknown but, as in palmar fibromatosis, trauma, neuropathy, faulty development, alcoholism, and infection have been proposed as etiologic factors. Pathogenesis in both palmar and plantar fibromatosis includes a genetic component, with family history and chromosome aberrations in 50% of the cases. Most lesions are located at the medial aspect and just superficial to the aponeurosis. Involvement is bilateral in 19% of patients and multiple in 32%. There is a higher prevalence in white and middle-aged (fourth decade) male patients and in patients who have epilepsy. There is also an association with knuckle pads in 5%, with palmar fibromatosis in 10–50%, and with penile fibromatosis (Peyronie disease) in 5–10% of patients. There are no reports of malignant transformation. Clinically, plantar fibromatosis presents as a nonmobile, irregular, single or multinodular lesion located in the longitudinal medial arch of the plantar surface of the foot. The lesion frequently consists of small nodules merged with each other and with the fascial bundles [4]. Although some authors report pain as a main symptom in one-third of patients, most lesions are asymptomatic and are discovered incidentally by palpation. Unlike palmar fibromatosis, this condition rarely causes contracture of the toes.

Microscopically, the lesion consists of a proliferation of well-differentiated hyperplastic, fibroblast-like cells or myofibroblasts with an infiltrative pattern of growth and usually an abundance of proliferating cells between the heavy strands of relatively hypocellular, mature collagen. Collagen is present in the actively growing foci in every specimen: quantitatively it usually is in an inverse ratio to the degree of cellularity [4]. Mitotic figures, necrosis, and vascular infiltration are uncommon. A cellular vascular cuffing and the presence of perivascular inflammatory cells have been described by Allen [4]. The natural history comprises a proliferative phase with increased fibroblastic activity and cellular proliferation, an involutional phase, and a residual phase in which fibroblastic activity is reduced and maturation of the collagen is noted.

If this condition is treated by simple excision, there is an recurrence rate of 50–65%, frequently resulting in a more aggressive form. Infiltration of neighboring structures is more frequently seen in recurrent lesions [4]. Wide, radical excision, encompassing 0.5 cm of surrounding, normal-appearing fascia is, therefore, the treatment of choice.

On ultrasound images, plantar fibromatosis is seen as a well-defined, hypoechoic nodule or mass superficial to the medial slip of the plantar aponeurosis. Plantar fibromatosis exhibits a consistent and characteristic appearance on MR images [61]. Most lesions are heterogeneous, with an overall SI equal to or slightly higher than that of muscle on both spin-echo T1- and (spin-echo and fast spin-echo) T2-weighted images (Fig. 13.11a, b). SI on T2-weighted images reflects the stage of the disease. The proliferative phase is characterized by higher cellularity, resulting in higher SI. The low SI on T2-weighted images of the involutional and residual phases is attributed to the hypocellularity and presence of abundant collagen. Lesions are slightly hyperintense to muscle on short-tau inversion recovery (STIR) sequences (Fig. 13.11c). After intravenous injection of Gd contrast, enhancement is inversely related to the stage of fibromatosis. "Burned out" lesions with abundant collagen fibers enhance to a lesser degree than lesions in the proliferative phase (Fig. 13.11e, f).

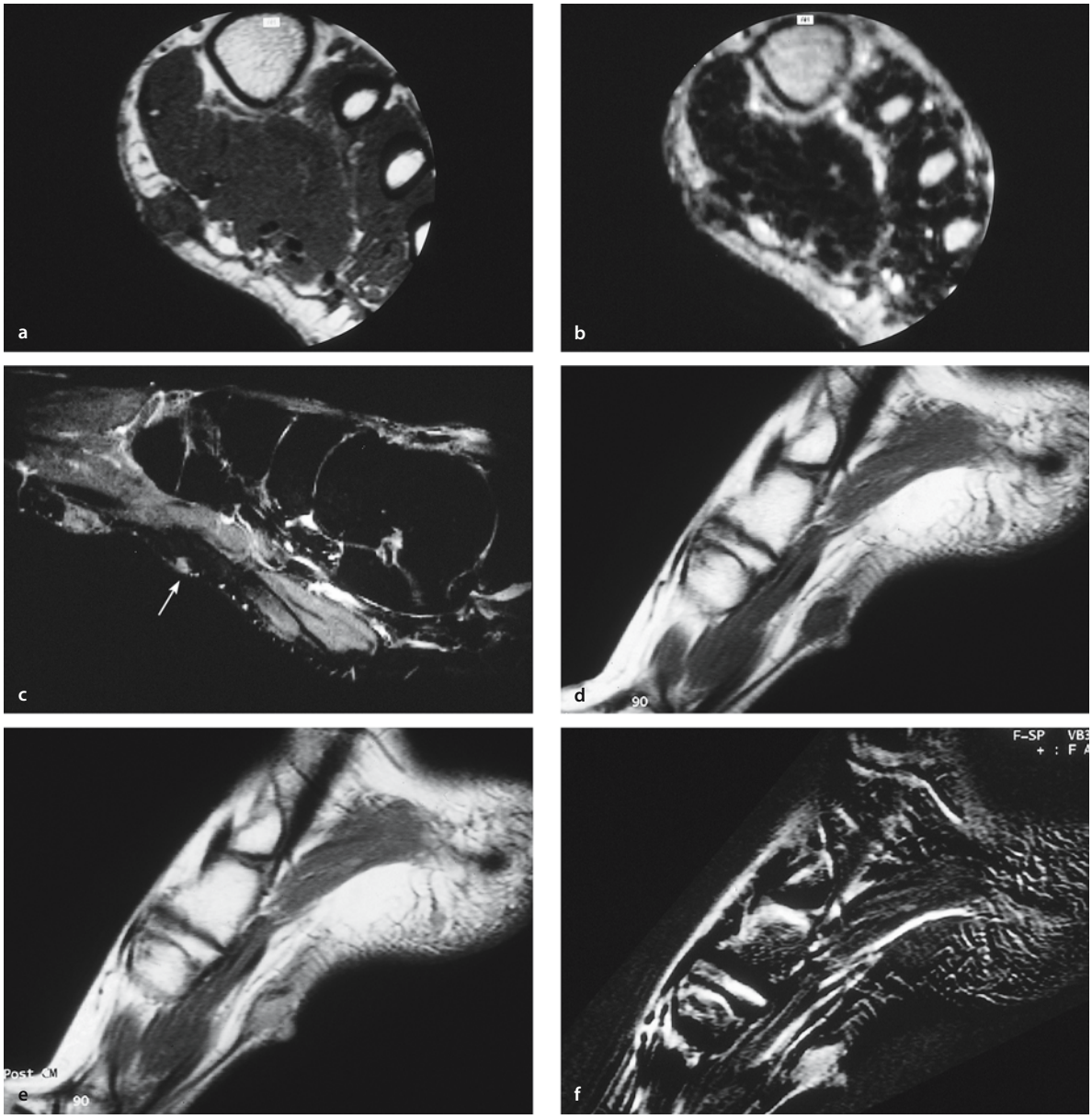

Fig. 13.11 a–f. Two cases of plantar fibromatosis in a 37-year-old-man (**a–c**) and in a 13-year-old girl (**d–f**). **a** Axial spin-echo T1-weighted MR image. **b** Axial turbo spin-echo T2-weighted MR image. **c** Sagittal STIR MR images. **d** Sagittal spin-echo T1-weighted MR image. **e** Sagittal spin-echo T1-weighted MR image after gadolinium contrast injection. **f** Sagittal subtraction MR image. Subcutaneous nodular lesion of intermediate signal intensity at the sole of the foot in apposition with the plantar aponeurosis. The lesion is isointense to muscle on the T1-weighted image (**a**), and of higher, variable signal intensity on the T2-weighted (**b**) and STIR (**c**) images. On the SRIR image, there is a smaller second lesion having similar signal characteristics (**c**; *arrow*). The second case reveals a lesion centered on the plantar fascia, isointense to muscle on the T1-weighted image (**d**), with marked enhancement after gadolinium contrast injection (**e**). This is also nicely demonstrated on the subtraction image (**f**)

Differential diagnosis has to be made between plantar fibromatosis in the residual phase, callus, and scarring. Since plantar fibromatosis in the proliferative phase may be an extremely cellular and infiltrative lesion, it has to be differentiated from aggressive fibromatosis and fibrosarcoma. If the lesion is associated with palmar fibromatosis or Peyronie disease, or if both feet are involved, the diagnosis is almost certain.

13.3.3 Knuckle Pads

Knuckle pads consist of a flat or dome-shaped fibrous thickening on the dorsal aspect of the proximal interphalangeal or metacarpophalangeal joints. They are frequently associated with palmar and plantar fibromatosis. Microscopically this condition resembles palmar fibromatosis, but there are no reports about knuckle pads in recent radiological literature.

13.3.4 Extra-abdominal Desmoid Tumors

Extra-abdominal desmoids are rare soft tissue tumors arising from connective tissue of muscle, overlying fascia, or aponeurosis. They have also been described as desmoid tumor, aggressive fibromatosis, or musculoaponeurotic fibromatosis. The term "desmoid" means band-like or tendon-like lesion [12].

The reported incidence of extra-abdominal desmoids is between three and four cases per million annually. The peak incidence is between ages 25 and 40 years. Although some authors report a predominance in women of childbearing age [16, 33], men and women are almost equally affected. Its cause is unknown, but surgical or accidental trauma, pregnancy, and estrogenic hormones are known associations. We have seen a recurrent desmoid tumor demonstrating an important increase in size (400%) during pregnancy, while most desmoids regress after the menopause [74].

The localization of a large number of extra-abdominal desmoids at the lateral aspect of the shoulder and the buttocks supports the idea of a posttraumatic etiology. The notion of an inherited defect in connective tissue formation is supported by some authors, and a genetic basis for at least some desmoid tumors is suggested by the familial Gardner syndrome, in which desmoid tumors, bony osteomas, dermoids and epidermoids, and/or nuchal fibromas coexist with abdominal wall desmoids, mesenteric desmoids, and intestinal polyposis [1, 78]. Some authors have hypothesized that an underlying mesenchymal defect may result in an imbalance in growth factors, resulting in multiple proliferative diseases, and may be responsible for the coexistence of desmoids, gastrointestinal polyps, and breast cancer [66].

Extra-abdominal desmoids arise most commonly in the lower limb or limb girdle and in the shoulder region. In cases of lower limb localization, a preference for the region of the sciatic nerve is reported [78]. Our own series consists of 30 extra-abdominal desmoid tumors in 26 patients. The localizations were as follows: head and neck region (n=1), upper limb (n=4), trunk (n=6), pelvis (n=8), and lower limb (n=11). Extra-abdominal desmoids never metastasize but multicentric, synchronous and metachronous presentation has been reported [77, 82]. In this condition, second tumor localizations generally develop proximally to the primary lesion. In our series, 5 of 26 patients had multiple localizations.

Bone involvement is not uncommon and has been reported in up to 37% of patients. In addition, primary intramedullary, juxtacortical, and periarticular desmoids are found, which are histologically indistinguishable from soft tissue desmoids. In the same way, bone desmoids can extend into the soft tissues just as soft tissue desmoids can involve bone [13].

Microscopically, extra-abdominal desmoids consist of elongated spindle-shaped cells (fibroblasts) of uniform appearance, surrounded and separated from each other by varying amounts of collagen. Dense collagen is found at the periphery, fibroblasts at the center [45]. Conversely, the center of the lesions may contain dense collagen, whereas the periphery may be composed of fibroblasts [78]. In addition, myxoid change, focal hemorrhage, increased vascularity, and focal inflammation may be seen [45]. Immunohistochemistry staining was positive for actin, consistent with myofibroblastic differentiation in extra-abdominal desmoid tumors [82] Despite their benign microscopic appearance, extra-abdominal desmoids have an aggressive behavior, which is expressed as large tumoral growth, infiltration of neighboring tissues, and a high incidence of postsurgical recurrence (between 25% and 68%). Most recurrent tumors have a different behavior and morphology. In our series they show an increased frequency of extracompartmental spread, grow considerably faster than primary tumors, and have a tendency to invade bone more frequently.

In a retrospective study of 138 patients with extra-abdominal desmoids, 11 died as a consequence of locally uncontrolled tumor growth [65]. Kim [40] has retrospectively analyzed the clinical records and MRI findings in 40 patients (8 juveniles, 32 adults) with proven desmoid tumor. In his series, recurrences in the juvenile patients were more often multiple (50% versus 12%) and appeared significantly earlier than in the adult patients.

On ultrasound scans, extra-abdominal desmoids may be well defined or poorly defined and may show variable echogenicity because of variable degrees of cellularity, matrix water content, and collagen. In many cases, marked shadowing from the surface of the lesion, a result of the large amount of dense collagen tissue in the tumor, totally obscures the mass [22].

Because of the variability in tumor composition, the lesions have variable attenuation and enhancement on CT scans [2]. Duda has reported that extra-abdominal desmoids are iso- or hypodense relative to muscle and enhance to 100–110 HU after injection of iodinated contrast material [14].

On MR images, the appearance of extra-abdominal desmoids varies [12, 64]. There are remarkable differences in shape in various patients as well as in different locations in a given patient with multicentric extra-ab-

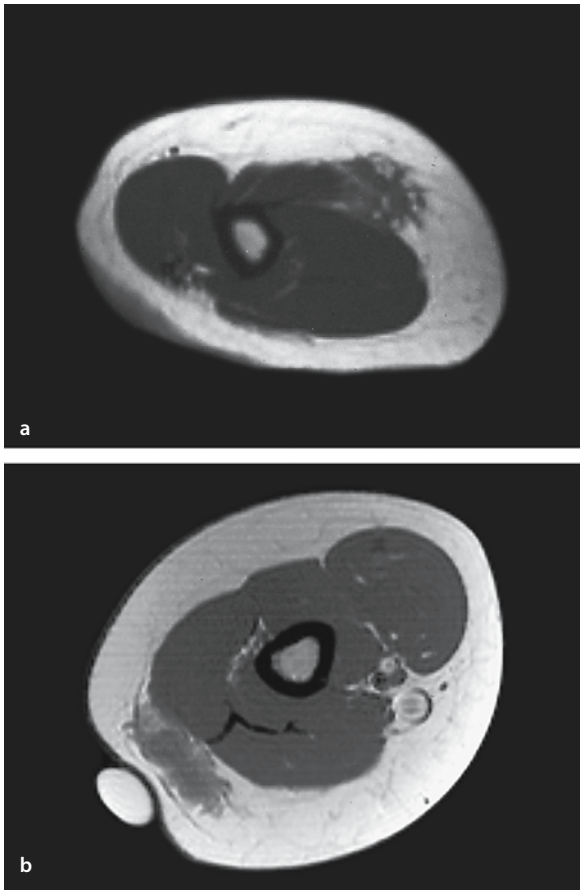

Fig. 13.12 a, b. Desmoid of the upper arm (**a**) in a 23-year-old woman and (**b**) in a 44-year-old woman. **a** Axial spin-echo T1-weighted MR image. **b** Axial spin-echo T1-weighted MR image after gadolinium contrast injection. In the first patient there is a stellar, infiltrating lesion within the subcutaneous fat of the deltoid region in close contact with the adjacent muscle fascia (**a**). In the second patient there is a stellar, nodular infiltrating lesion within the subcutaneous fat of the deltoid region. The fat plane between the lesion and the adjacent muscle fascia is blurred (**b**). These two cases of superficial, stellar desmoid in the deltoid region with infiltration of neighboring fat and muscle fascia illustrate the characteristic shape and location of superficial aggressive fibromatosis

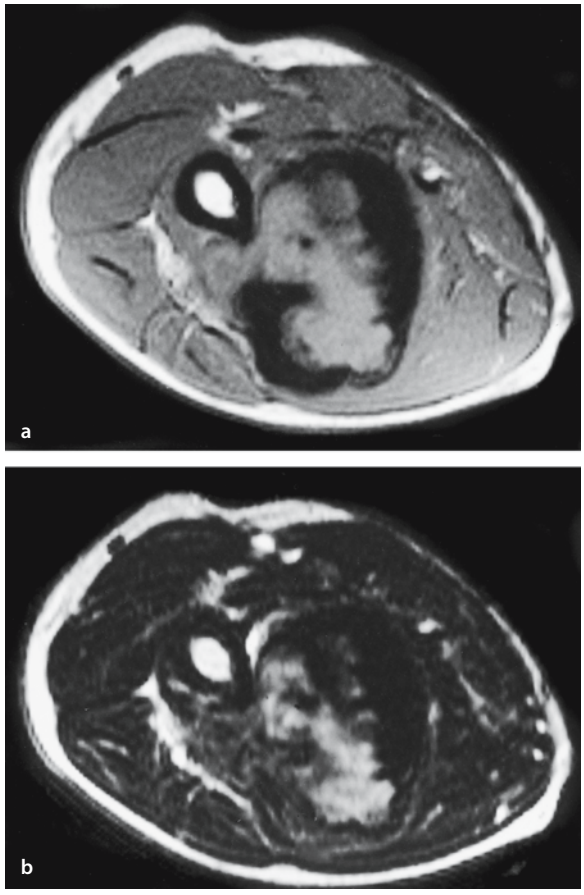

Fig. 13.13 a, b. Desmoid of the forearm in a 71-year-old man. **a** Axial spin-echo T1-weighted MR image. **b** Axial spin-echo T2-weighted MR image. On the T1-weighted image, there is a large mass at the volar aspect of the forearm adjacent to the interosseous membrane, with a rim of low signal intensity at the periphery of the lesion (**a**). On the T2-weighted image, the peripheral rim remains hypointense while the central part is of higher signal intensity (**b**). This case illustrates a pattern of natural evolution where dense collagen is responsible for low signal intensity at the periphery of the lesion on all pulse sequences

dominal desmoids. Likewise, for a given lesion, shape may vary on follow-up examinations. The infiltrative pattern is significantly more common in juvenile patients (63%), whereas the nodular pattern is more frequent in the adult patients (81%) [40]. In our series, the shape of the lesions was fusiform-ovoid or dumbbell, and irregular or stellate when located in the subcutis (Fig. 13.12). The mean maximum diameter was 72 mm.

In the reported cases, extra-abdominal desmoids appear hypo- or isointense to muscle on spin-echo T1-weighted images. SI on T2-weighted images is mostly intermediate, although very low and extremely high signal intensities have been noted occasionally. Low-SI, patchy, linear or curvilinear areas on T2-weighted images correspond to hypocellular tissue and dense collagen. On both spin-echo sequences, but predominantly on T2-weighted images, extra-abdominal desmoids are inhomogeneous, mostly with higher SI in the central part (cellular) than at the periphery (collagenous) [33, 45] (Figs. 13.13–13.16).

After a retrospective study of 36 patients with histologically proven extra-abdominal desmoids, Hartman et al. have concluded that on MR images, the desmoids showed inhomogeneous SI (97%), poor margination (89%), neurovascular involvement (58%), and bone involvement (37%). Fibrosis was present in 88% of primary desmoids and 90% of recurrent lesions, and intermediate SI (greater than that of muscle and lower than that of fat) was present in 75% and 50% of these, respectively [32].

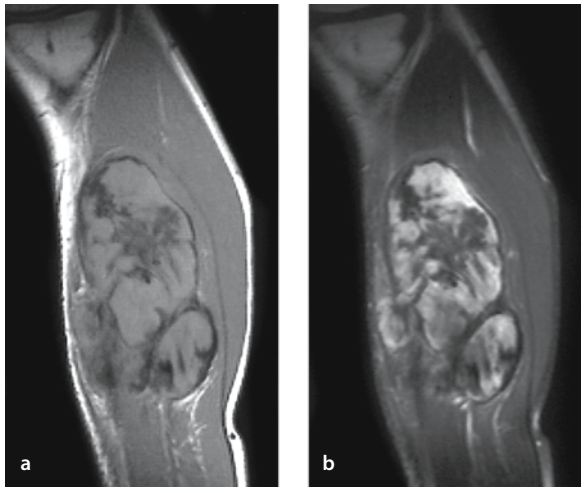

Fig. 13.14 a, b. Desmoid of the calf in a 23-year-old man. **a** Sagittal spin-echo T2-weighted MR image. **b** Sagittal spin-echo T1-weighted MR image after gadolinium contrast injection. On the T2-weighted image, there is a polylobular mass with central areas of low signal intensity within each nodule and presence of a low signal-intensity capsule around the lesion (**a**). After contrast injection there is marked enhancement of the peripheral zones without enhancement of the central scar-like areas (**b**). This case of deeply seated juxtacortical desmoid (adjacent to the dorsal aspect of the tibial cortex) illustrates another pattern of natural evolution where collagen is found in the center and less collagenous parts at the periphery of the lesion. Furthermore, it illustrates a frequent finding that areas of higher signal intensity on T2-weighted images enhance after gadolinium administration, whereas areas of low signal intensity on T2-weighted images do not enhance and remain hypointense on all pulse sequences

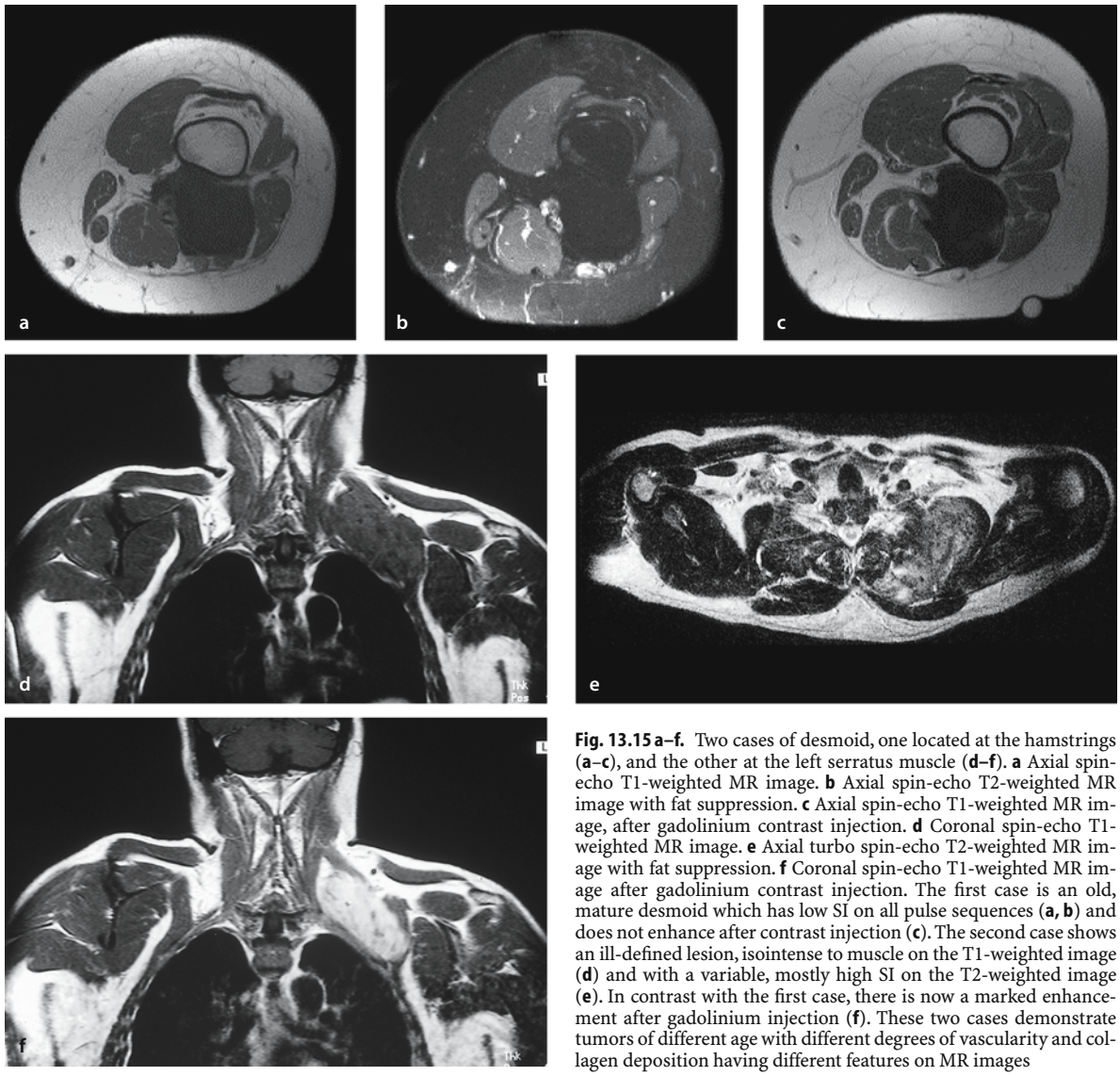

Fig. 13.15 a–f. Two cases of desmoid, one located at the hamstrings (**a–c**), and the other at the left serratus muscle (**d–f**). **a** Axial spin-echo T1-weighted MR image. **b** Axial spin-echo T2-weighted MR image with fat suppression. **c** Axial spin-echo T1-weighted MR image, after gadolinium contrast injection. **d** Coronal spin-echo T1-weighted MR image. **e** Axial turbo spin-echo T2-weighted MR image with fat suppression. **f** Coronal spin-echo T1-weighted MR image after gadolinium contrast injection. The first case is an old, mature desmoid which has low SI on all pulse sequences (**a, b**) and does not enhance after contrast injection (**c**). The second case shows an ill-defined lesion, isointense to muscle on the T1-weighted image (**d**) and with a variable, mostly high SI on the T2-weighted image (**e**). In contrast with the first case, there is now a marked enhancement after gadolinium injection (**f**). These two cases demonstrate tumors of different age with different degrees of vascularity and collagen deposition having different features on MR images

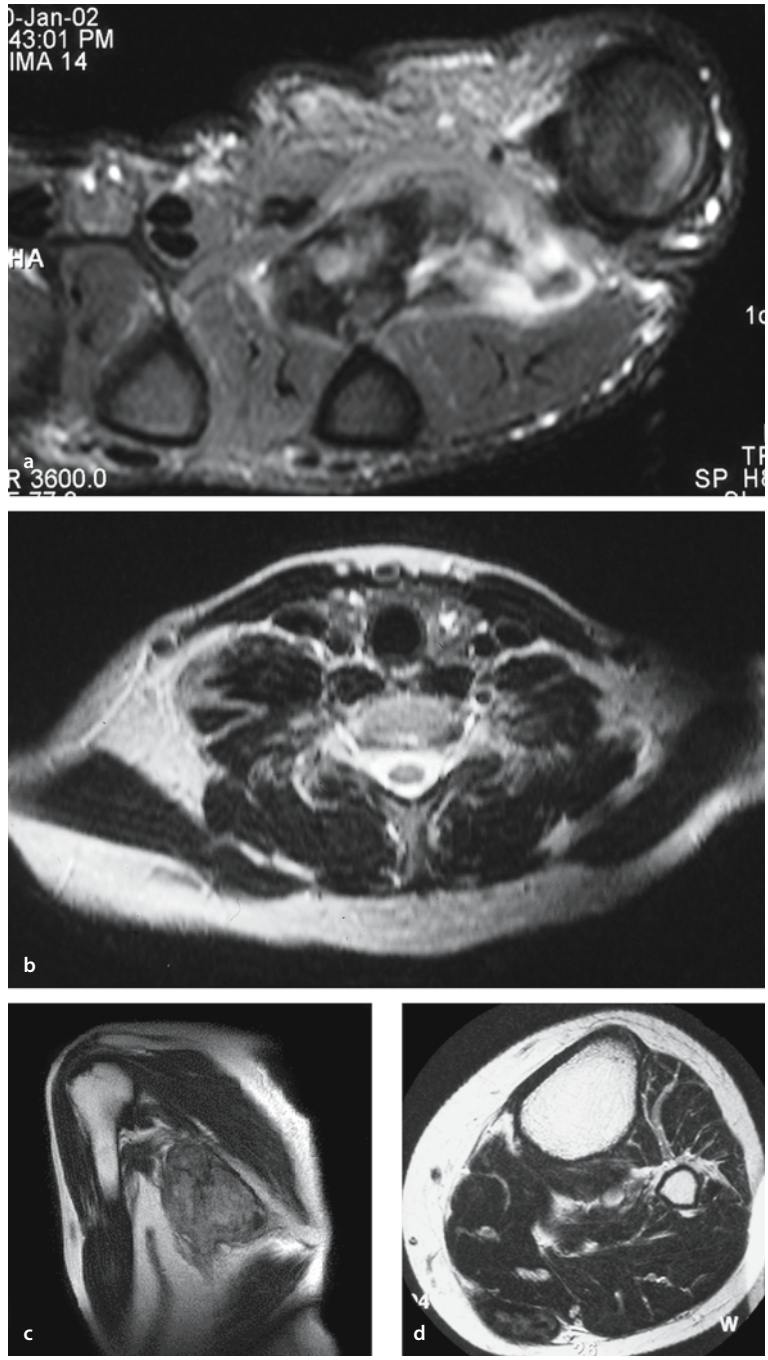

Fig. 13.16 a–d. Four different cases of desmoid tumor showing their most characteristic feature, i.e., nonhomogeneity and low SI on T2-weighted MR images

In our personal study of 30 desmoid tumors, MR signal characteristics were variable. On T1-weighted images, lesions were usually almost homogeneous or homogeneous (n=25). The overall SI was rated as equal to SI of muscle in 21 cases. The SIs on T2-weighted images mostly were heterogeneously distributed (n=24), with an overall SI slightly lower than (n=15) or equal to (n=8) fat. Hypointense areas were mostly curvilinear to irregular and may have a central (n=4) or peripheral (n=3) distribution within the lesion. Two cases with central low-intensity areas also show a low-SI peripheral band. The low-SI areas mostly comprise 0–20 % of the lesion (n=14).

There are few reports regarding the use of contrast agents in extra-abdominal desmoids. In our series, all desmoid tumors showed a moderate to strong enhancement on spin-echo Gd T1-weighted images, except for the areas of low SI on T2-weighted images, which re-

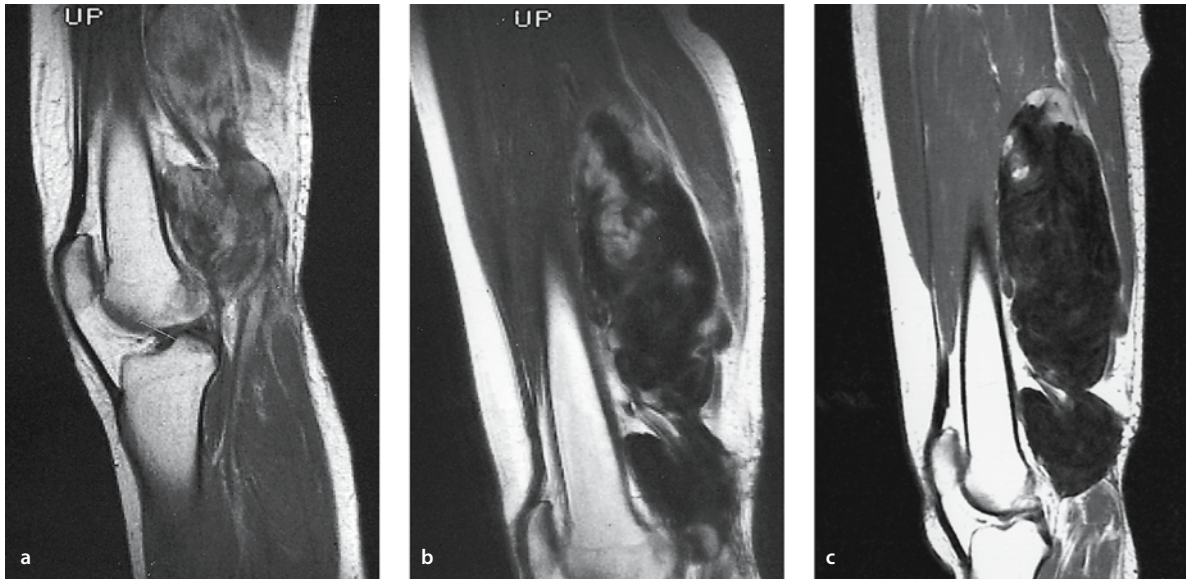

Fig. 13.17 a–c. Desmoid of the popliteal fossa in a 28-year-old woman. **a** Sagittal spin-echo T1-weighted MR image after gadolinium contrast injection (January 1989). **b** Sagittal spin-echo T1-weighted MR image after gadolinium contrast injection (November 1991). **c** Sagittal spin-echo T1-weighted MR image after gadolinium contrast injection (April 1994). The MRI examination from 1989 shows a large, dumbbell-shaped mass in the popliteal fossa with marked, nonuniform enhancement of 80% of the lesion (**a**). In 1991, the proximal part of the mass had increased in size, while the size of the distal part had decreased. Limited areas (20% of the lesion) of enhancement in the proximal part and no enhancement in the distal part (**b**). On the image from MRI performed in 1994, there is no further change in tumor size. Except for two small enhancing nodules within the top of the proximal lesion (5% of the lesion), the whole mass remains hypointense after contrast injection (**c**). This case illustrates the natural evolution of a primary desmoid tumor over a period of 6 years, showing the proximal migration of the lesion and the gradual decrease in enhancing cellular areas, together with an increase in nonenhancing collagenous components

mained unenhanced. Enhancement was more pronounced in the areas of high SI on spin-echo T2-weighted images. As a result, inhomogeneity was even better demonstrated on spin-echo Gd T1-weighted images (Figs. 13.12, 13.14, 13.15). On follow-up examinations, the inhomogeneous pattern of contrast enhancement became more evident and paralleled the changes in SI noted on spin-echo T2-weighted images.

In cases of multicentric presentation, the distal lesion tended to be more heterogeneous and hypointense on T2-weighted images than the proximal one. Since the low SI of extra-abdominal desmoids on spin-echo T2-weighted images is thought to be a consequence of an increased amount of collagen, we presume that in these cases the distal localization is more collagenous than the proximal one.

On follow-up MR examination, the distal lesions showed a tendency to shrink, as may be concluded from their size and progressive serration of their borders. In contrast, the proximal lesions increased with time and became more convex. Moreover, during follow-up examination, the extent of the hypointense areas in the distal lesions increased, and this was associated with a further decrease in SI on spin-echo T2-weighted images.

The same phenomenon has been described by Feld in a patient with multicentric involvement in which a gluteal lesion manifested low SI on T2-weighted images, whereas a lesion in the psoas muscle showed heterogeneous, increased SI on T2-weighted images. Histological examination of the gluteal lesion revealed dense collagenous bundles, with cellular areas comprising less than 20% of the tumor, while the lesion in the psoas muscle showed less collagenization and a more pronounced cellularity [19].

The amount of collagen in a given lesion may be reflected by SI on spin-echo T2-weighted images. This correlation between amount of collagen and SI on spin-echo T2-weighted images suggests that older localizations of extraabdominal desmoids (mature fibromatosis) show an increase in collagen that suggests progressive fibrosis, while, in cases of multicentric presentation, the proximal lesion seems to be less collagenous compared with the distal one (Fig. 13.17).

The relationship between cellularity and SI on T2-weighted images, as described by several authors [14, 19], could not be confirmed in our own series. Subtle changes in cellularity cannot explain substantial variance in SI on T2-weighted images, and, although there is a difference in cellularity between young and older

desmoids and between primary and recurrent ones, the overall cellularity of desmoids is low. Differences in SI between different tumor components, between asynchronous multicentric desmoids, and between primary and recurrent desmoids will therefore be a consequence of a combination of variability in cellularity, amount of collagen, water content of the extracellular space, myxoid substance, and vascularity.

Periarticular desmoid tumors have to be differentiated from other lesions with low SI on T2-weighted images, such as pigmented villonodular synovitis, giant cell tumor of the tendon sheath, hemorrhagic synovitis, and hemophilic arthropathy [88]. Differential diagnosis of subcutaneous desmoids includes other superficial fibromatoses, such as nodular fasciitis, injection granulomas, granuloma annulare, pentazocine-induced myopathy with subcutaneous fibrosis, and postsurgical fibrosis [10, 80].

13.3.5 Abdominal Fibromatosis (Abdominal Desmoids)

Abdominal desmoids are rare fibroblastic lesions commonly found within the musculoaponeurotic fascia of the anterior abdominal wall, especially of the rectus and oblique external muscles. Occasionally they grow eccentrically and present as an intra-abdominal tumor. Seventy percent of cases occur in patients between the second and fourth decades, and they are common in women. There is a definite relationship with pregnancy (during or after), abdominal surgery, and trauma. It has been postulated that these tumors are estrogen sensitive. Abdominal desmoids may occur as isolated lesions or may be seen as a manifestation of Gardner syndrome.

Abdominal desmoid tumors are well-defined lesions, 5–15 cm in diameter, and in rare cases contain calcifications, necrotic or cystic changes, or hemorrhagic components. If they originate in the rectus muscle they do not cross the midline of the abdomen. On CT scans, most abdominal desmoids are well defined and homogeneous and appear isodense or slightly hypodense with respect to muscle. If lesions are hyperdense, this is due to the high density of abundant collagen and the rich capillary network [16]. The majority of lesions are either isodense or hyperdense when compared with muscle on contrast-enhanced scans.

On MR images, tumors show nonspecific high SI on T2-weighted images, while low-SI areas on T2-weighted images probably represent abundant fibrous tissue [36] (Fig. 13.18). Despite adequate resection with clear histological margins, the recurrence rate may be as high as 40%. Sifumba has reported a tumor recurrence during pregnancy in an old scar 9 years after resection of a first abdominal desmoid [76].

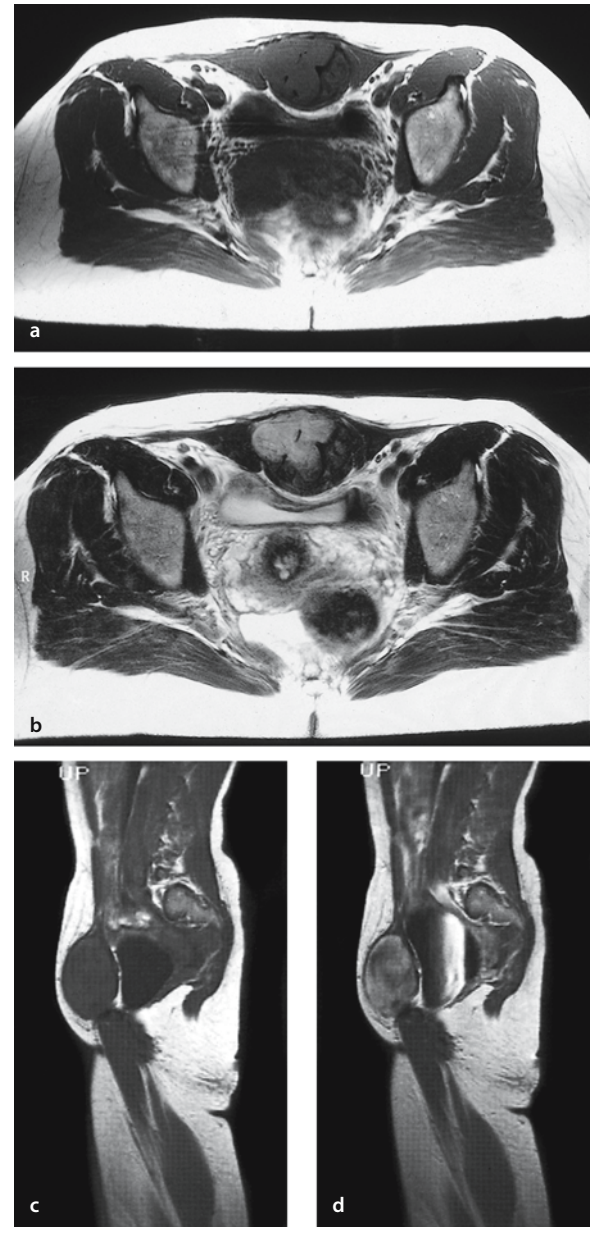

Fig. 13.18 a–d. Abdominal desmoid in a 50-year-old woman (**a, b**) and in a 22-year-old woman (**c, d**). **a** Axial spin-echo T1-weighted MR image. **b** Axial turbo spin-echo T2-weighted MR image. **c** Sagittal spin-echo T1-weighted MR image. **d** Sagittal spin-echo T1-weighted MR image after gadolinium contrast injection. A polylobular mass can be seen, isointense to muscle and with low signal intensity septations on the T1-weighted image (**a**). On the T2-weighted image, the lesion has a mixed, overall low signal intensity (**b**). The second case involves the rectus muscle in a woman in the postpuerperal period. On the T1-weighted image, there is a well-delineated fusiform, inhomogeneous mass within the rectus muscle, with signal intensity comparable with signal intensity of muscle (**c**). The lesion demonstrates marked, nonuniform enhancement (**d**). These cases are illustrative of abdominal desmoids with characteristic location, patient age, and time of onset (postpuerperal)

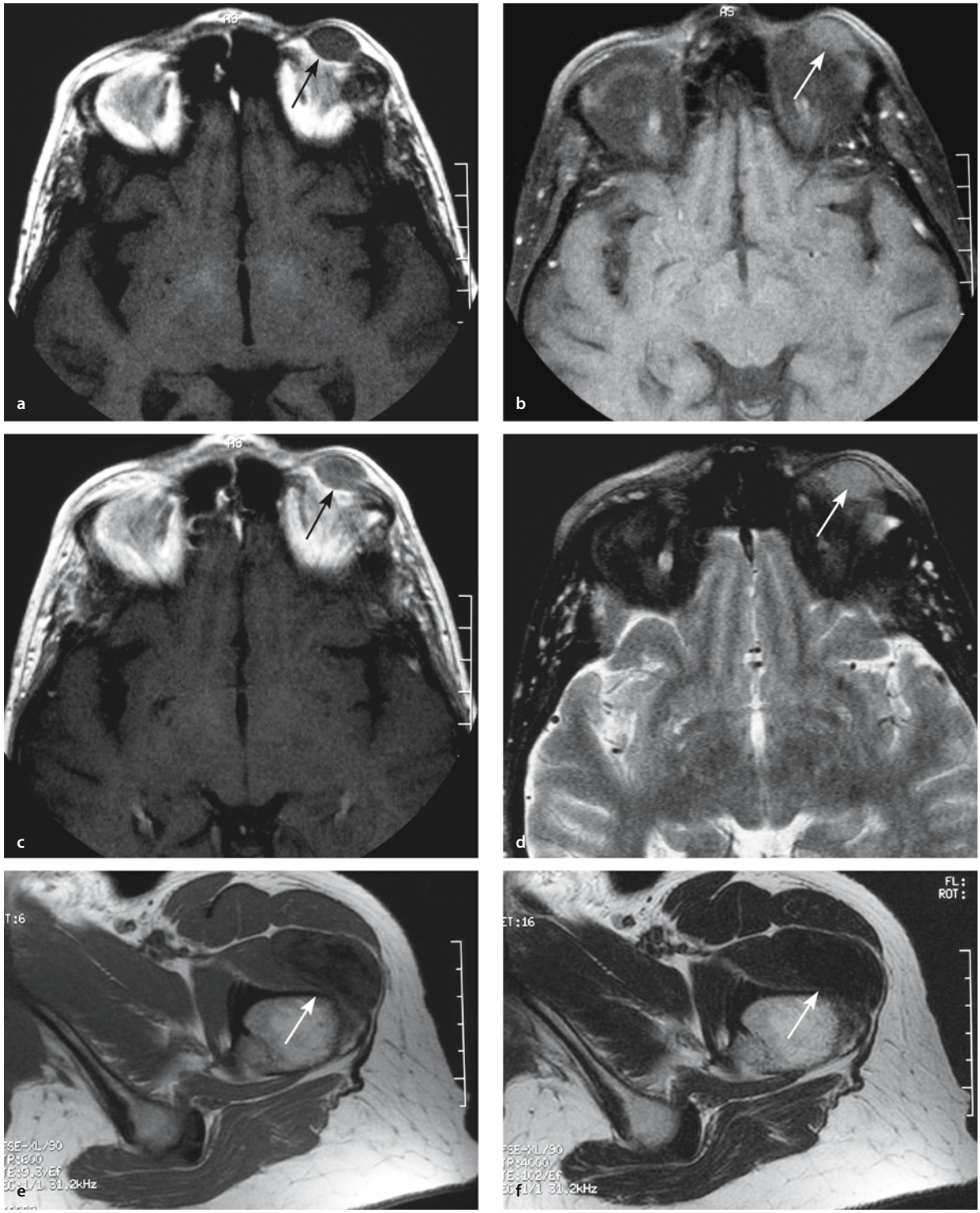

Fig. 13.19 a–g.

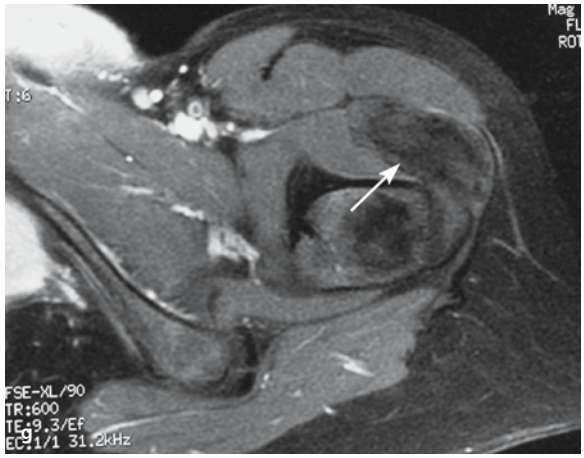

Fig. 13.19 g. Two cases of collagenous fibroma, one in the subcutis (**a**–**d**) and a second in the vastus muscle (**e**–**g**). **a** Axial spin-echo T1-weighted MR image. **b** Axial spin-echo T1-weighted MR image with fat suppression. **c** Axial spin-echo T1-weighted MR image, after gadolinium contrast injection. **d** Axial spin-echo T2-weighted MR image. **e** Axial spin-echo T1-weighted MR image. **f** Axial spin-echo T2-weighted MR image. **g** Axial spin-echo T1-weighted MR image, after gadolinium contrast injection. Morphology and MR presentation doesn't allow differentiation between collagenous fibroma and extra-abdominal desmoid

13.3.6 Collagenous Fibroma (Desmoplastic Fibroblastoma)

Collagenous fibroma commonly occurs in patients in the fifth and sixth decades of life, more frequent in men (75%). The tumor often manifests as a sharply demarcated, mobile, firm, solitary mass involving subcutaneous tissue, or skeletal muscle. The common locations of the tumor are the arm, shoulder, and posterior neck or upper back. The size of reported collagenous fibromas range from 1 to 20 cm in the largest dimension. Histologically, the tumors appear well marginated on low-power examination. The tumor cells are relatively bland stellate- and spindle-shaped fibroblastic cells separated by densely fibrous to fibromyxoid matrix. The cellularity is low or very low, mitotic figures are very rare or absent, and tumor necrosis is not seen. On MR images collagenous fibroma shows areas of decreased SI on T1- and T2-weighted images. Because both have a high collagen content, similar findings have been described in desmoid tumors (Fig. 13.19).

Nevertheless, collagenous fibromas are less cellular, less vascular, and less infiltrative at their periphery and as a consequence more mobile, better circumscribed, and easier to remove than desmoids. Moreover they occur in older (more than 40 years old) patients. Differential diagnosis is essential to prevent overtreatment in collagenous fibroma [63].

13.4 Fibrous Tumors of Infancy and Childhood

The following types of fibrous tumors of infancy and childhood are recognized:

1. Fibrous hamartoma of infancy
2. Infantile digital fibromatosis
3. Infantile myofibromatosis
4. Juvenile hyaline fibromatosis
5. Gingival fibromatosis
6. Fibromatosis colli
7. Infantile (desmoid-type) fibromatosis (aggressive infantile fibromatosis)

The term "fibromatosis" is used for fibroblastic-myofibroblastic proliferations with the following characteristics: (a) a tendency to invade surrounding tissues, (b) a tendency to recur after incomplete resection, (c) absence of metastases, (d) in some fibromatoses, spontaneous regression, and (e) presentation with multifocal tumors [15].

13.4.1 Fibrous Hamartoma of Infancy

Fibrous hamartoma of infancy is a solitary, benign, painless, subcutaneous tumor occurring before the age of 2 years and characterized by an organoid mixture of three components: trabeculae of dense fibrocollagenous tissue, areas of immature-appearing, small, rounded, primitive mesenchymal cells, and mature fat. The lesion occurs predominantly in males. The most common locations are the shoulder, axilla, and upper arm [17, 53]. There is a strong correlation between the imaging findings and the histological pattern showing fat and fibrous tissue (Fig. 13.20).

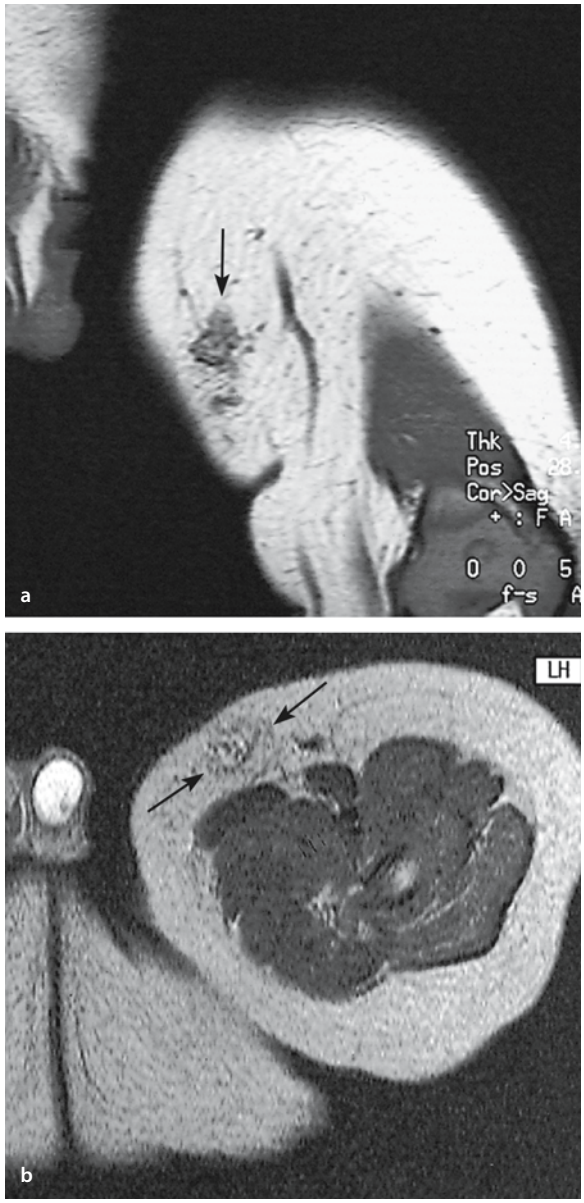

Fig. 13.20 a, b. Fibrous hamartoma in a 6-month-old boy. **a** Coronal spin-echo T1-weighted MR image. **b** Axial spin-echo T2-weighted MR image. On the T1-weighted image, the lesion presents as an ill-defined, inhomogeneous mass of intermediate signal intensity within the subcutaneous tissue of the ventral aspect of the left thigh (**a**). On the T2-weighted image, the lesion is spider-like, with low to intermediate signal intensity (**b**). MRI demonstrates the histological composition with fatty and fibrous parts

13.4.2 Infantile Digital Fibromatosis – Inclusion-Body Fibromatosis

In infantile digital fibromatosis, single or multiple fibromatous lesions arise from the fingers and toes, affecting predominantly the dorsolateral aspect of the distal parts of adjacent digits. This rare entity mostly develops in patients under the age of 3 years, and histological examination typically reveals intracytoplasmatic inclusion bodies [37].

13.4.3 Infantile Myofibromatosis

Infantile myofibromatosis, also called congenital multiple or diffuse fibromatosis, is a rare mesenchymal disorder in newborns and infants, which is characterized by solitary or multiple nodular foci of myoblastic and fibroblastic tissue in the skin, musculoskeletal system, and visceral organs. The condition is also known as multiple mesenchymal hamartomas or multiple vascular leiomyomas of the newborn, and infantile hemangiopericytoma. Its etiology is unknown, although familial occurrence of the disease has been noted.

According to the anatomical distribution of the myofibroblastic lesions, two types of infantile myofibromatosis can be distinguished, each with a different clinical course. The first (solitary) type is limited to soft tissue and bone and has an excellent prognosis, since spontaneous regression with complete resolution of the lytic bone lesions may occur. It is mostly found in boys. Most solitary myofibromas occur in cutaneous/subcutaneous tissues of the head and neck region. The second (multicentric) type shows widespread visceral involvement, mainly of the lungs, myocardium, and gastrointestinal tract. This type of myofibromatosis is almost always lethal in early life. It is mostly found in girls [84].

Subcutaneous nodules are usually firm and encapsulated, and frequently contain calcifications. They are the most common manifestations of infantile myofibromatosis and are easily detectable at birth. Tumors measure from less than 1 cm to a few centimeters in diameter. They contain foci of hemorrhage, cystic degeneration, necrosis, calcification, ossification, and fat [15]. Histologically nodular lesions consist of fusiform spindle cells and cells of intermediate differentiation between fibroblasts and smooth muscular cells, called myofibroblasts. Immunocytochemical staining is positive for vimentin and smooth muscle actin, and negative for desmin.

Plain films and CT scans show a low-density soft tissue tumor developing within muscle or subcutaneous tissue and containing calcifications (Fig. 13.21). After contrast injection, there is a homogeneous enhancement [6]. Eich [15] describes the MR appearance of infantile myofibromatosis: they are isointense to muscle

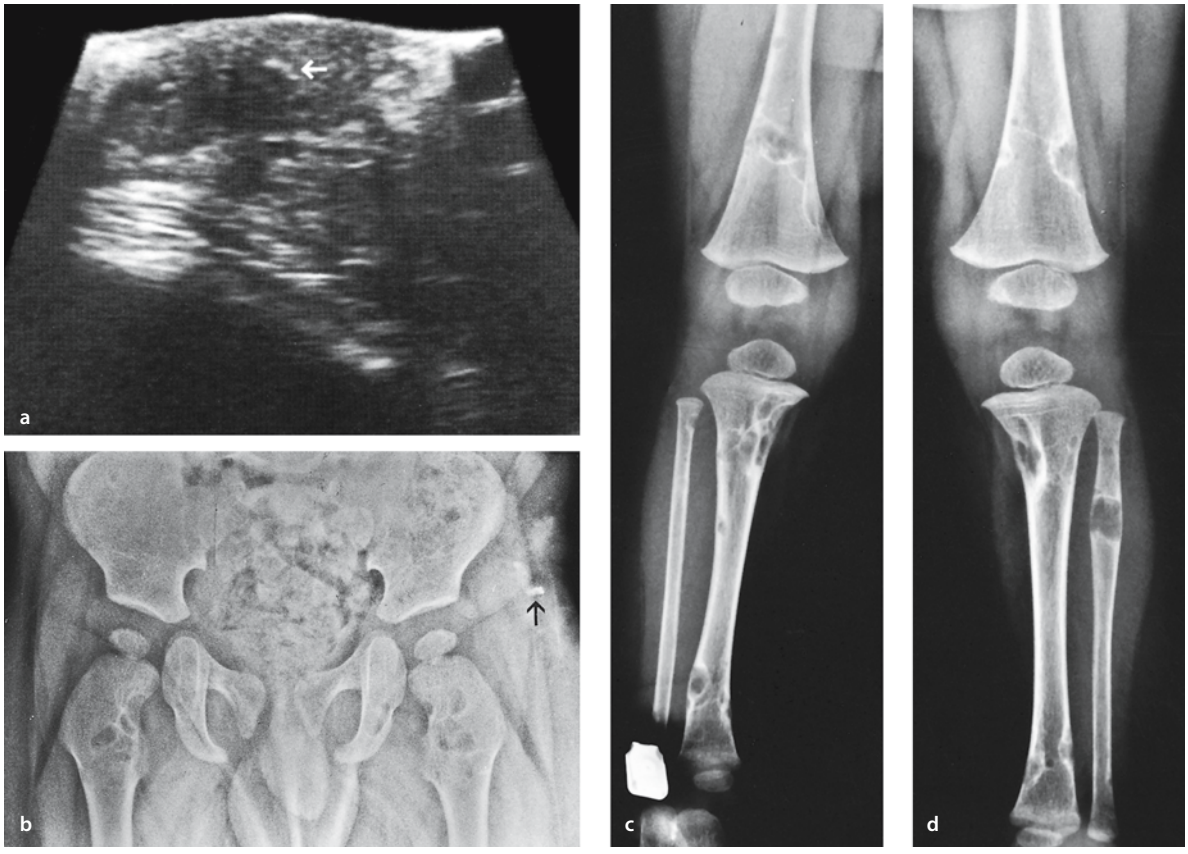

Fig. 13.21 a–d. Infantile myofibromatosis in a 10-month-old boy. **a** Ultrasound. **b** Radiograph of the pelvis, anteroposterior view. **c, d** Radiographs of both legs. On an ultrasound scan (**a**) there is a solid, echoic oval mass with a small central hyperechoic focus suggesting calcification (*arrow*). Radiography of the pelvis (**b**) reveals a calcification in the soft tissue lateral to the left acetabulum (*arrow*). There are symmetrical, multiloculated osteolytic lesions in both proximal femora and ischial bones. The lesions are sharply defined and have sclerotic margins. Radiographs of both legs (**c, d**) show multiple, rounded and ovoid, lytic metaphyseal lesions in the femur, tibia, and fibula bilaterally. They all have an intracortical localization and sclerotic margins. The lesion in the proximal left fibula is slightly expansile. In this case, the age of the patient and the coexistence of bone and soft tissue lesions are indicative of infantile myofibromatosis. Follow-up demonstrated spontaneous regression and even disappearance of the lesions. (By courtesy of W.G. Wassenaar, Afdeling Radiodiagnostiek, Academisch Ziekenhuis Nijmegen St. Radboud, Geert Grooteplein 18, Postbus 9101, 6500 HN Nijmegen, The Netherlands [84])

on T1-weighted images, hyperintense to muscle on T2-weighted images, and strongly enhancing after contrast injection. Some of the lesions in his series show a characteristic target-sign appearance on MR images, the center of these lesions being mildly hyperintense on T1-weighted images and nonenhancing. Recently Koujouk [44] has described MR findings in six cases consisting of low SI on T1-weighted MR images, target appearance with high- or low-SI center on T2-weighted MR images, and peripheral enhancement after contrast administration. Skeletal involvement is seen in the skull, spine, chest, shoulder girdle, pelvis, and extremities. Within the tubular bones, lesions are located predominantly in the metaphyseal region, centrally or eccentrically. Lesions are lytic, sharply marginated, and sometimes expansile. Although a characteristic radiological appearance of widespread lytic bone lesions associated with calcified soft tissue nodules is noted, differential diagnosis of multiple myofibromas should include fibrous dysplasia, neurofibromatosis, and lymphangiomatosis; while solitary myofibroma should include traumatic myositis ossificans, juvenile aponeurotic fibroma, and soft tissue chondroma [79].

13.4.4 Juvenile Hyaline Fibromatosis

Juvenile hyaline fibromatosis is a rare condition that is thought to be a mesenchymal dysplasia, showing multiple subcutaneous tumors, hypertrophic gingiva, and flexion contractures of the extremities. Calcifications in soft tissue tumors, scoliosis, marked osteopenia, well-defined osteolytic lesions and cortical defects in tubular bones, severe acro-osteolysis, and destruction of epiphyses of the long bones are also reported (Fig. 13.22). This autosomal, recessive condition is reported in chil-

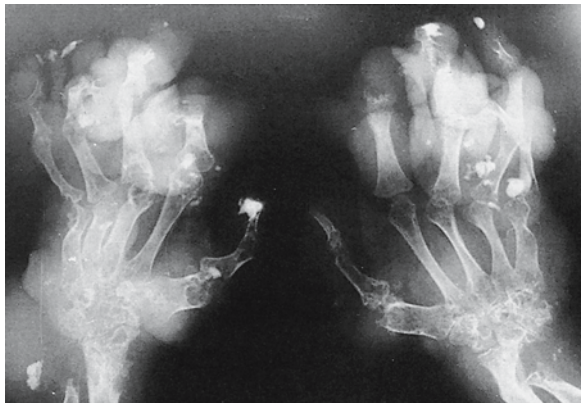

Fig. 13.22. Juvenile hyaline fibromatosis in a 36-year-old woman. Radiograph of the hands. There are multiple, calcified soft tissue nodules and expansile osteolytic lesions in the tubular bones, with marked deformation of the wrists and small joints. Severe acro-osteolysis. (Reproduced from [28], with permission)

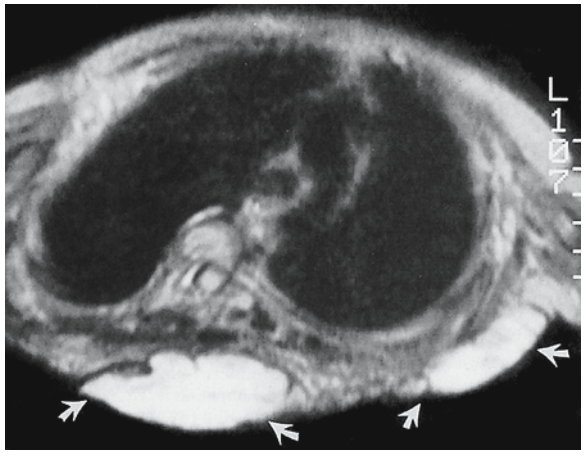

Fig. 13.23. Juvenile hyaline fibromatosis in a 9-year-old girl with multiple palpable nodules throughout the body and severe scoliosis. Axial spin-echo T2-weighted MR image of the trunk Presence of two large subcutaneous masses showing extremely high signal intensity on the T2-weighted image. In this case of juvenile hyaline fibromatosis, the bright signal on the T2-weighted image is consistent with the presence of hyaline matrix. (Reproduced from [38], with permission)

dren of consanguineous parents, and clinical onset occurs between 2 months and 4 years of age. Subcutaneous nodules are slow growing and may reach a large size, producing great deformities. Surgical excision is often followed by tumor recurrence.

Histologically the lesion is characterized by the presence of hyaline substance in the tumoral connective tissue. Diagnosis is confirmed by electron-microscopic examination [28]. On MR images the lesions are bright on T2-weighted images, most likely reflecting the hyaline matrix which is characteristic of the lesions (Fig. 13.23). MRI may be a significant diagnostic aid, as other fibromatosis syndromes have nodules that are of low signal on T2-weighted images [38].

13.4.5 Fibromatosis Colli

Fibromatosis colli is a peculiar growth of the sternocleidomastoid muscle that appears within the 1st weeks of life and is often associated with torticollis. It occurs in 0.4% of newborns. There is a marked male predominance. It remains unclear whether the fibroblastic proliferation is reparative or neoplastic. Although there is a history of breech or complicated delivery in more than 4% of the cases, microscopic appearance of the lesion differs from that of proven cases of organizing hematoma, and there is also very little demonstrable hemosiderin within it. Vascular impairment as the result of prolonged venous stasis or ischemia during labor is another possible cause. Nevertheless there is a clear association with other musculoskeletal developmental abnormalities that are associated with abnormal intrauterine positioning, including forefoot anomalies and congenital hip dislocation [20].

Clinically the lesion manifests between the 2nd and 4th week of life as a firm mass of 2–3 cm diameter lying within the lower portion of the sternocleidomastoid muscle. Initially it grows rapidly, but after a few weeks or months, growth comes to a halt. Later it begins to regress and may disappear after a period of 1 or 2 years. It never recurs and at no time does it behave aggressively. During the initial growth period, torticollis occurs in 40% of all cases and usually is mild and transient.

Microscopically the sternocleidomastoid muscle is partially replaced by a fibroblastic process of varying cellularity without pleomorphism or mitotic activity. Residual degenerated muscle fibers are intimately mixed with proliferated fibroblasts. Long-standing lesions may show a lower degree of cellularity and a greater amount of stromal collagen [17].

On ultrasound scans, the mass within the belly of the sternocleidomastoid muscle is spindle shaped and may be hyperechoic (50%), isoechoic, or hypoechoic relative to normal muscle. The echotexture may be homogeneous (50%) or heterogeneous (50%). The mass is surrounded by a hypoechoic rim in 90% of cases [1]. Ultrasound is the method of choice for follow-up of fibromatosis colli (Fig. 13.24b) [9]. On CT scans, fibromatosis colli appears as a focal or diffuse isodense enlargement of the sternocleidomastoid muscle with or without mass effect (Fig. 13.24a). On MR images fibromatosis colli may present with a slightly increased SI on T2-weighted images compared with normal muscle (Fig. 13.24c, d) or with a slightly decreased SI on T2-weighted images consistent with the presence of some fibrous tissue [1]. Imaging findings that are not characteristic of fibromatosis colli are: mass extending beyond

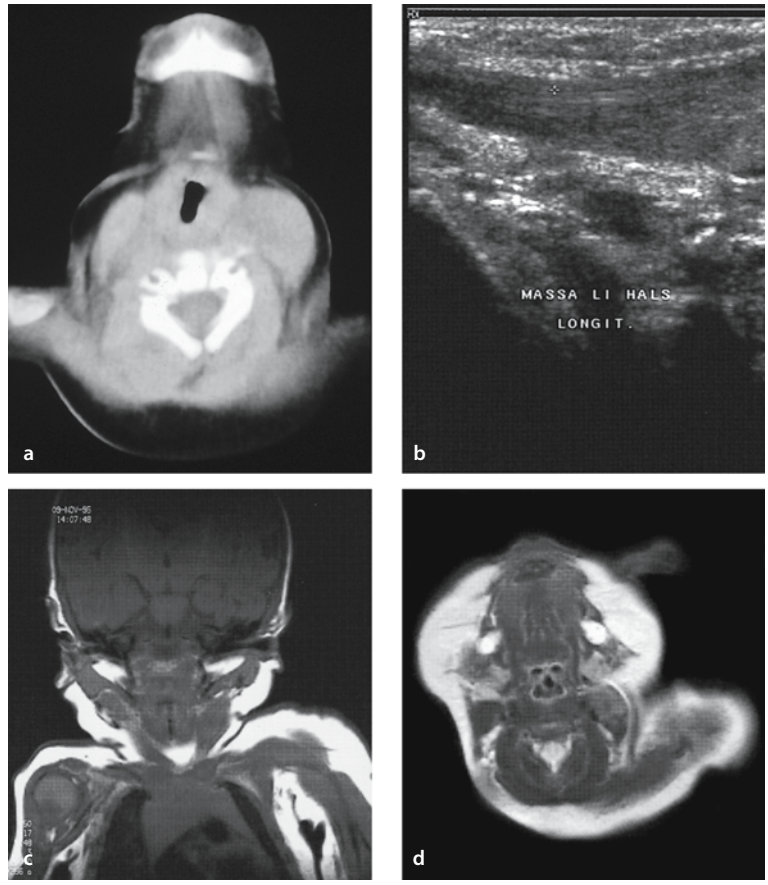

Fig. 13.24 a–d. Fibromatosis colli in a 1-day-old boy (**a**) and a 7-week-old girl (**b–d**) presenting clinically with torticollis. **a** CT scan. **b** Ultrasound of the left sternocleidomastoid muscle. **c** Coronal spin-echo T1-weighted MR image. **d** Axial turbo spin-echo T2-weighted MR image. CT scan showing overall enlargement of the left sternocleidomastoid muscle, without obvious change in attenuation (**a**). On ultrasound scans, there is a fusiform mass in the distal part of the muscle. The mass is hyperechoic and lacks muscle fiber structure (**b**). On the T1-weighted image, there is a fusiform enlargement of the left sternocleidomastoid muscle (**c**), while on the T2-weighted image the lesion is less homogeneous and predominantly of high signal intensity (**d**). Characteristic age, location, and shape of a fibroma colli

the margins of the sternocleidomastoid muscle, poor definition of the surrounding fascial planes and/or mass associated with adenopathy, bone involvement, intracranial or intraspinal extension, vascular encasement, and airway compression. If essential clinical and radiological features of fibromatosis colli are present, recognition of this entity by medical imaging can prevent unnecessary diagnostic and therapeutic maneuvers [9].

13.4.6 Infantile (Desmoid-Type) Fibromatosis

Infantile (desmoid-type) fibromatosis represents the infantile variety of musculo-aponeurotic desmoid-type of fibromatosis. Infantile fibromatosis may occur in bone, in soft tissues or in a generalized form (soft tissues, viscera, and bone) Lesions mostly occur in the head and neck region. They appear as nodular, rounded, or oval masses with well-defined margins or as more infiltrative, permeative lesions with indistinct borders extending to encase adjacent neurovascular structures and bone [41]. Most lesions are unifocal at presentation; when multifocal they also show intra-abdominal mesenteric and retroperitoneal spread and ascites. Familial cases occur, particularly as part of Gardner syndrome [15]. If bony lesions coexist they are purely lytic lesions with an aggressive appearance [86].

Although histologically benign, the lesion tends to gradually infiltrate soft tissues (skin, subcutaneous tissues, muscles, and even tendons, nerves, and blood vessels) and adjacent bone – hence the terms aggressive juvenile fibromatosis, juvenile or infantile fibrosarcoma, congenital fibrosarcoma, desmoplastic fibrosarcoma of infancy, and medullary fibromatosis of infancy [73]. These terms are used for all fibroblastic tumors of infancy that show an abundant number of cells and prominent mitotic activity [86]. Aggressive infantile fibromatosis is usually first detected at birth or within the first 3 months of life. Col [8] has reported on the observation of a fetal tumor on antenatal echography which was diagnosed after birth as aggressive fibromatosis of the trunk. There is no sexual predilection. The condition occurs most frequently in the skeletal muscle or in adjacent aponeuroses of the extremities in the head and neck, shoulder and upper arm, and the thigh. A case of aggressive infantile fibromatosis of the thigh which subsequently metastasized to the lungs has been reported by Shankwiler [73].

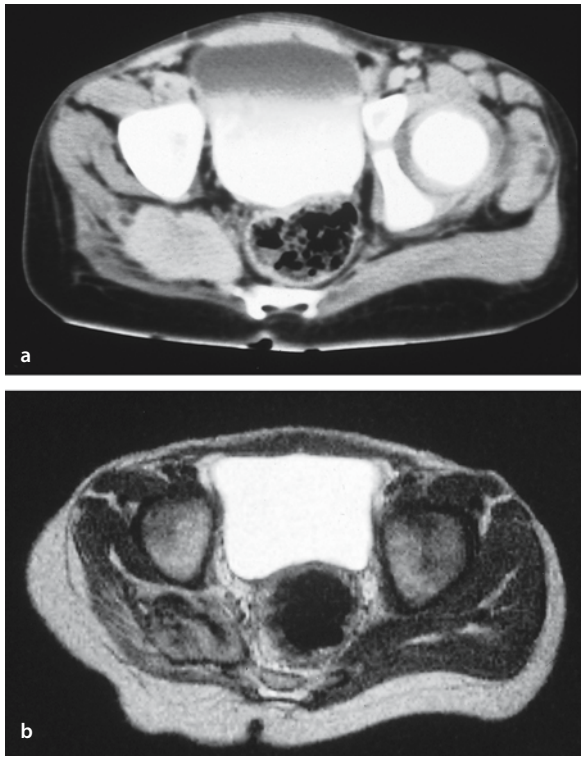

Fig. 13.25 a, b. Infantile fibromatosis in a 2-year-old boy. **a** CT scan. **b** Axial turbo spin-echo T2-weighted MR image. Slowly growing mass in the right gluteal region, with uncharacteristic CT attenuation (**a**). Note the atrophy of adjacent gluteal muscles. On the T2-weighted image, the lesion is of mixed, overall low signal intensity. While the lesion is nonspecific on CT scan, it has a characteristic low signal intensity on the T2-weighted MR image as a consequence of its high collagen content

Microscopically, two patterns can be distinguished that reflect progressive stages in the differentiation of fibroblasts. The immature type is composed of cells which are intermediate in appearance between primitive mesenchymal cells and fibroblasts, and are associated with a dense meshwork of reticulin fibers and considerable amounts of mucoid material. The mature type is composed of more mature fibroblasts associated with varying amounts of collagen. It closely resembles adult musculo-aponeurotic fibromatosis. Aggressive juvenile fibromatosis lesions are hypercellular and composed of pleomorphic, mitotically active, spindle-shaped fibroblasts arranged in a herringbone pattern [73].

Only a few cases of infantile fibromatosis have been reported with uncharacteristic appearance on ultrasound and CT scans, i.e., homogeneous and hypoechoic on ultrasound, and homogeneous, hyper-, or isodense with respect to muscle on precontrast CT scans, enhancing after contrast administration [51]. Extensive ossification within an infantile fibromatosis is a rare finding, which has been described by Fromowitz [26].

The variable MR imaging signal characteristics of infantile desmoid fibromatosis reflect differences in composition, especially cellularity, fibrous tissue content, and the presence of myxomatous degeneration. Most desmoid tumors are heterogeneous soft-tissue lesions of intermediate SI (between those of muscle and fat). Lesions may be hypointense, isointense, or, occasionally, marginally hyperintense with respect to muscle signal on T1-weighted images and of mixed, predominantly high signal (greater than that of muscle but usually less than that of fat) on T2-weighted images. Zones of low SI are often seen on both T1- and T2-weighted images. The difference in T2-weighted SI appears to be determined by the degree of cellularity rather than the amount of collagen present in the lesion (Fig. 13.25). After IV injection of Gd contrast, tumors may show homogeneous, inhomogeneous, or no significant enhancement. No relationship has been shown between the pattern of enhancement and tumor recurrence.

13.5 Intermediate-Grade Fibromyoblastic Tumors

In the new WHO classification, this group contains the extrapleural solitary fibrous tumor, inflammatory myofibroblastic tumor, hemangiopericytoma, and infantile fibrosarcoma.

13.5.1 Solitary Fibrous Tumor

Solitary fibrous tumor is a mesenchymal tumor of probable fibroblastic type which shows a prominent, hemangiopericytoma-like branching vascular pattern. It's an uncommon lesion observed in middle-aged adults without sex predilection. It can be found at any location of which 40% in the subcutaneous tissue. Most solitary fibrous tumors are found at the pleura, face, and meninges. It is mostly a large, well delineated, slowly growing and painless mass. Histopathologically it consists of a mixture of hypocellular and hypercellular areas separated from each other by thick bands of collagen and branching, hemangiopericytoma-like vessels. Malignant solitary fibrous tumors (10–15%) behave aggressively and show histopathological features of hypercellularity, cytological atypia, necrosis, numerous mitoses, and infiltrative growth.

On MR images, solitary fibrous tumors of the extremities have nonspecific features, i.e., inhomogeneous, low to intermediate SI on T1-weighted images and inhomogeneous, intermediate to high SI on T2-weighted images [3] (Fig. 13.26).

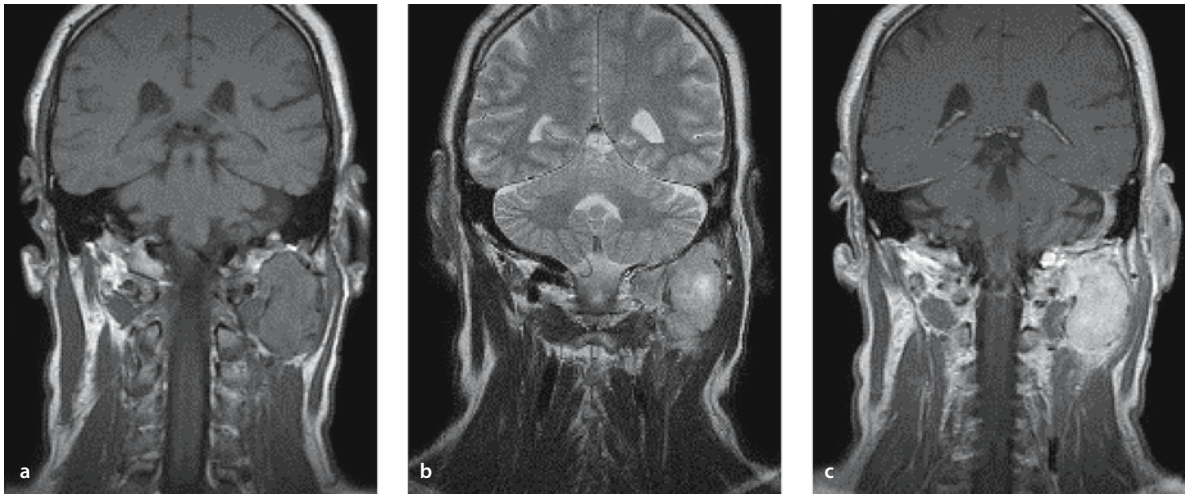

Fig. 13.26 a–c. Solitary fibrous tumor. **a** Coronal spin-echo T1-weighted MR image. **b** Coronal spin-echo T2-weighted MR image. **c** Coronal spin-echo T1-weighted MR image, after gadolinium contrast injection. Mass lesion in between the left sternocleidomastoid muscle and deep cervical muscles, presenting with low to intermediate SI on both T1- (**a**) and T2-weighted (**b**) MR images and with marked enhancement after contrast administration (**c**)

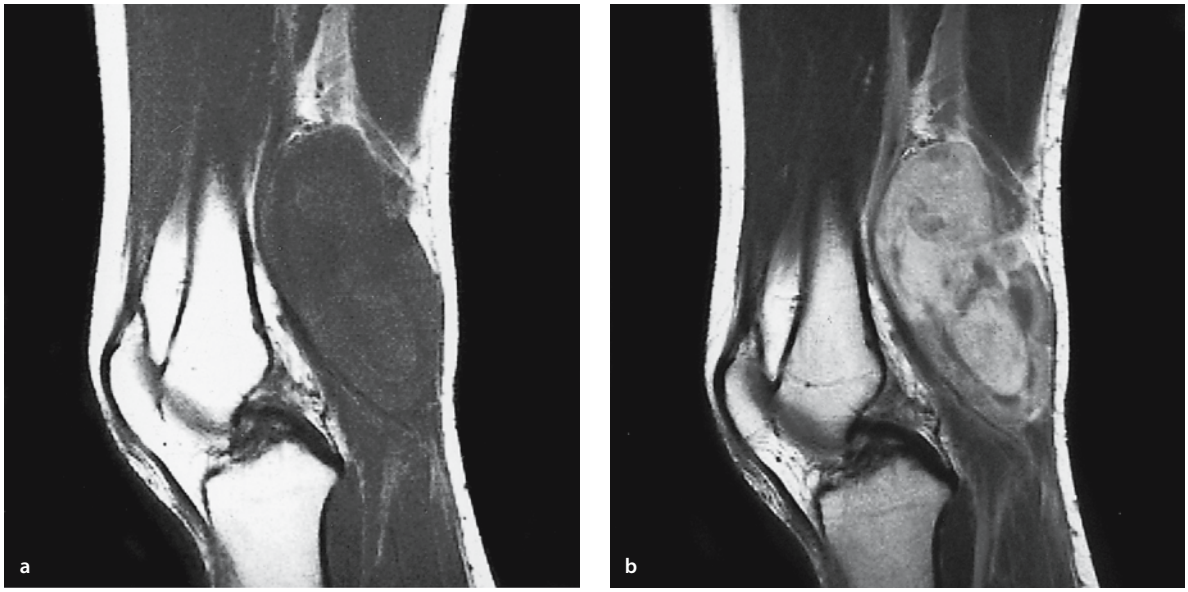

Fig. 13.27 a, b. Hemangiopericytoma of the right popliteal fossa. **a** Sagittal T1-weighted MR image. **b** Sagittal T1-weighted MR image after gadolinium contrast injection. An oval, largely homogeneous lesion is seen lying superficial to the major vessels. There is no invasion of the subcutis (**a**). After contrast administration, a strong enhancement of the mass is seen (**b**)

13.5.2 Hemangiopericytoma

Hemangiopericytoma is a slow growing tumor of intermediate grade of malignancy that never metastasizes (Fig. 13.27). The term is used to encompass a wide variety of neoplasms which have in common the presence of a thin-walled, branching vascular pattern. They most commonly occur in middle-aged adults, with an apparent female predominance. The pelvis and retroperitoneum are the most frequent locations.

Histopathologically hemangiopericytoma closely resembles solitary fibrous tumor, albeit with the consistent presence of numerous, variably ectatic or compressed, thin-walled branching vessels, often having a staghorn configuration [20].

13.5.3 Inflammatory Myofibroblastic Tumor

It is a distinctive lesion, primarily a visceral and soft tissue tumor of children and young adults, composed of myofibroblastic spindle cells accompanied by an inflammatory infiltrate of plasma cells, lymphocytes and eosinophils. All body parts can be affected and they determine the symptoms of inflammatory myofibroblastic tumor [20]. Lung, mesentery omentum, and orbits are the most common sites.

Findings of a mass lesion are frequently in association with fever, weight loss and pain. Imaging studies reveal a lobulated, solid mass which can be inhomogeneous. Intralesional calcifications are described.

In our own series we have one case of an inflammatory myofibroblastic tumor located in the subcutis with infiltration of the underlying fascia. The lesion is ill defined with nonspecific MR features, i.e., low SI on T1-, and high SI on T2-weighted MR images and peripheral enhancement after contrast administration.

13.5.4 Infantile Fibrosarcoma

Infantile, congenital or juvenile fibrosarcoma is a rare childhood malignancy (3% of all childhood tumors) of mesodermal origin. (Fig. 13.28) For some authors [17], infantile fibrosarcoma is a distinct lesion, while for others [73, 81] it cannot be differentiated from the aggressive infantile type of fibromatosis described above. It usually presents at birth or during the first year of life. Prenatal diagnosis is likely to increase with the advent of routine antenatal ultrasound. There is no sex preponderance. The superficial and deep soft tissues of the extremities, especially distally, are the most common sites, accounting for 61% of cases overall. [20] It tends to show a rapid increase in size and distant metastasis may occur in 8% of cases [34]. Infantile cases are often grotesquely large in proportion to the size of the child [20] Adjacent bone may show some deformity with cortical thickening and failure of normal tubulation. Large tumors may cause bone erosion, bowing, remodeling, or destruction. Intratumoral ossification or calcification is rare.

Histologically, infantile fibrosarcoma is an undifferentiated fibroblastic spindle cell tumor of intermediate grade of malignancy, which is densely cellular, often in a herringbone pattern with numerous mitoses and infiltrative margins. Collagen formation is not prominent. Cystic, myxoid, highly vascular, and necrotic tumor components are often seen [34]. Histological description parallels that of an aggressive juvenile fibromatosis (see Sect. 13.4.6). Tumors are isoechoic on US and mild-

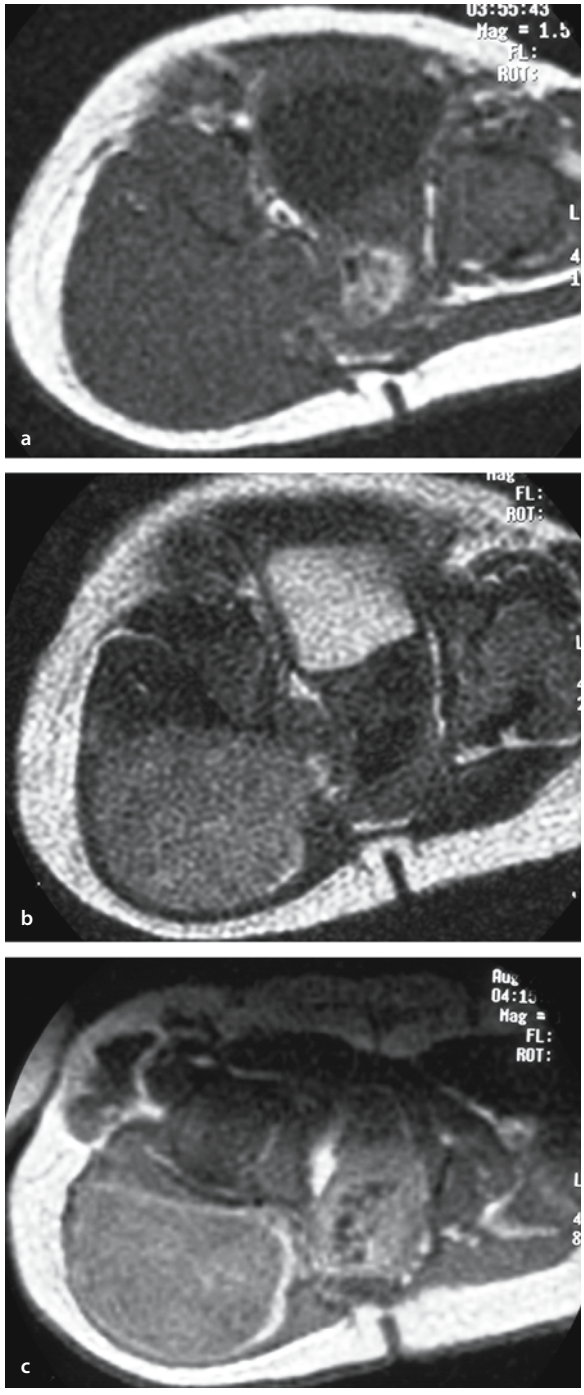

Fig. 13.28 a–c. Infantile fibrosarcoma. **a** Axial spin-echo T1-weighted MR image. **b** Axial turbo- T2-weighted MR image. **c** Axial spin-echo T1-weighted MR image after gadolinium contrast injection. Infantile fibrosarcoma at the right gluteal region presenting with nonspecific MR features, i.e., low SI on T1- (**a**), and intermediate SI on T2-weighted images (**b**). There is moderate enhancement after contrast administration (**c**)

ly hypodense on plain CT. On MR, they appear isointense on T1-weighted images and hyperintense on T2-weighted images. There is an heterogeneous enhancement pattern with low SI areas, both centrally and in the periphery of the lesions [15].

CT is useful in demonstrating the extent of the tumor and the bony involvement, while disruption of soft tissue planes is better shown on MR images. MRI has a role in follow-up and early detection of local tumor recurrence. Use of Gd contrast agents may aid in differentiating between fibrosis and tumor recurrence [81].

13.6 Malignant Fibromyoblastic Tumors

13.6.1 Adult Fibrosarcoma

Adult fibrosarcoma is a malignant tumor composed of fibroblasts with variable collagen production and herring-bone architecture and is capable of recurrence and metastasis [17]. Histologic, immunohistochemical, and ultrastructural examination are important tools for diagnosing fibrosarcoma and for differentiating fibrosarcoma from nodular fasciitis, myxofibrosarcoma, musculoaponeurotic fibromatosis, and other sarcomas. Recognition of these lesions as specific tumors and entities is responsible for the decline in the incidence of fibrosarcoma and for the overdiagnosis of fibrosarcoma in earlier studies.

Clinically, fibrosarcoma presents as a slowly growing, solitary, palpable mass with a diameter of 3–8 cm. It may reach a large size before causing symptoms. The lesion is most common between the ages 30 and 55 years, and the incidence is slightly higher in women. The thigh and the knee region are preferential localizations, followed by the trunk, distal legs, and forearms. Less than 5% present in the head and neck [29]. Deep fibrosarcomas originate from the intramuscular and intermuscular fibrous tissue, fascial envelopes, aponeuroses, and tendons. They may cause periosteal and cortical thickening, and rarely demonstrate intralesional calcifications or ossifications. Superficial or subcutaneous

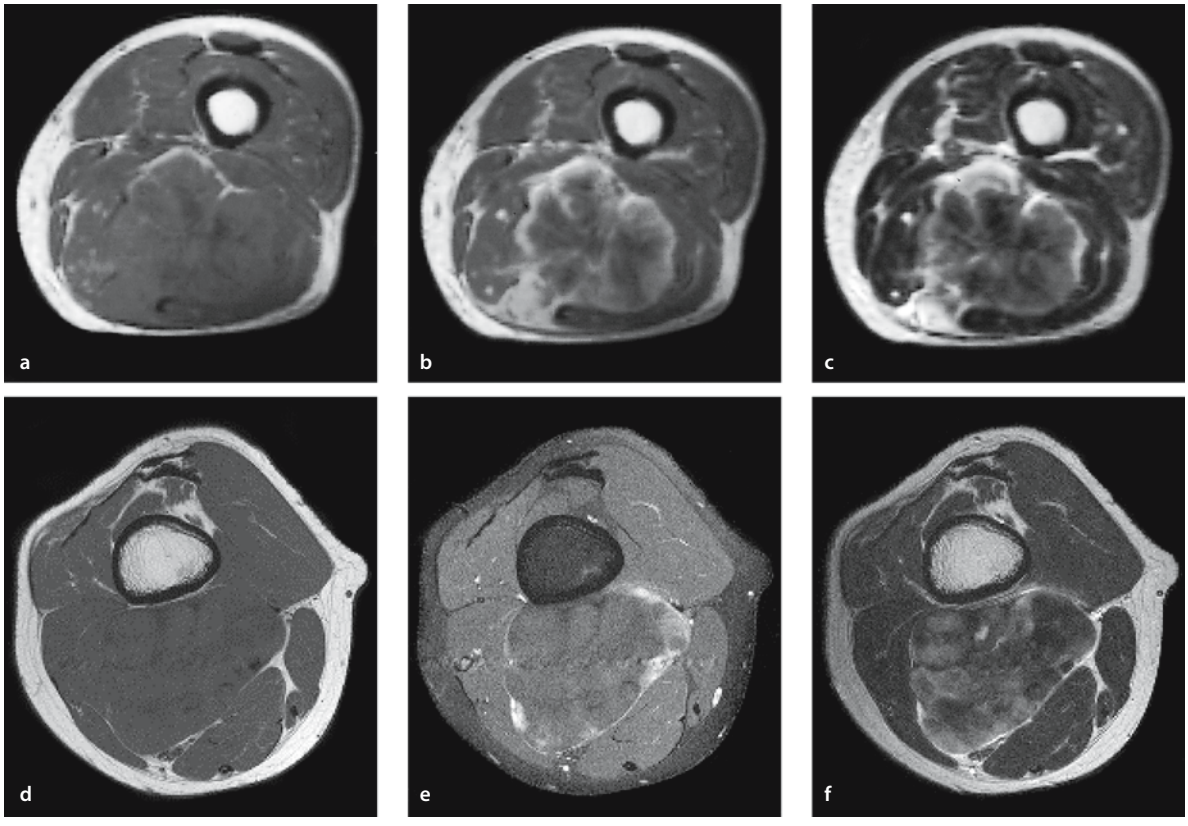

Fig. 13.29 a–f. Two cases of Fibrosarcoma (**a–c, d–f**). **a** Axial spin-echo T1-weighted MR images. **b** Axial spin-echo T1-weighted MR images after gadolinium contrast injection. **c** Axial spin-echo T2-weighted MR images. **d** Axial spin-echo T1-weighted MR images. **e** Axial spin-echo T1-weighted MR images after gadolinium contrast injection, with fat suppression. **f** Turbo spin-echo T2-weighted MR images. In both cases lesions are nonhomogeneous and isointense to muscle on T1-weighted MR images (**a**, **d**), they are nonhomogeneous and of overall low SI on T2-weighted MR images (**b**, **e**) and enhance in a spoked-wheel pattern after contrast administration (**c**, **f**). Large size and SIs are compatible with the diagnosis of fibrosarcoma. Good delineation and speckled areas of low SI do not allow differentiation from extra-abdominal desmoids

fibrosarcomas arise in tissues damaged by trauma, scarring, heat (burns), or radiation.

Macroscopically, small fibrosarcomas are well defined, while larger fibrosarcomas tend to be poorly defined, grow in a diffusely invasive manner, and are often multiloculated. Microscopically, fibrosarcomas have a rather uniform or fasciculated growth pattern consisting of spindle-shaped cells separated by interwoven collagen fibers that are arranged in a parallel fashion. Mitotic activity is a condition for diagnosis. Grading of fibrosarcoma (well differentiated versus poorly differentiated) is based on the degree of cellularity, cellular maturity, the amount of collagen produced by the tumor cells, and the presence of necrosis and/or intralesional hemorrhage.

Low-grade fibrosarcoma (well differentiated) is defined by sheets of uniform spindle cells with moderate cellularity arranged in a herringbone pattern, mild nuclear pleomorphism, and only rarely mitoses. A collagenous stroma is usually present. High-grade lesions (poorly differentiated) show greater nuclear pleomorphism, abundant cellularity, frequent mitotic activity, and possible tumor necrosis. Despite the fact that desmoids are characterized more by their localization and that fibrosarcomas are larger in size, differentiation between desmoids (representing more than 70% of tumors of fibrous tissue) and fibrosarcomas (less than 5%) is difficult even on MR images (Figs. 13.29, 13.30). Multicentric presentation of fibrosarcoma is a rare finding which can hardly be differentiated from metastatic fibrosarcoma (Fig. 13.31). The treatment of choice is wide local excision. Simple excision of fibrosarcomas is often followed by local recurrence.

Medical imaging literature about fibrosarcoma is sparse and limited to case reports. In our series of soft tissue tumors, we had nine cases of primary fibrosarcoma and two recurrent fibrosarcomas. The age range of patients was between 16 and 77 years, with a mean age of 47 years. In contrast to results reported in the literature, nine of ten patients were men. Nine lesions were located on the lower limb, from the groin to the sole of the foot. One patient presented with multiple bone and soft tissue localizations. Diameters were between 2 and 27 cm (mean diameter, 12 cm).

All patients underwent MRI. Lesions were either homogeneous or inhomogeneous on both T1- and T2-weighted images. Most lesions showed signal intensities equal to those of muscle on T1-weighted images and low-SI areas on a background of moderate to high SI on T2-weighted images. T1-weighted images after Gd contrast were performed in nine patients. Ninety percent of the lesion showed a marked, peripheral enhancement, with a spoked-wheel appearance in three patients. Nonenhancement of central tumor parts was not a consequence of intratumoral necrosis. In only one case did the nonenhancing central part correspond to an area of high SI on T2-weighted images. Osseous involvement was rare, being noted only once in the group of solitary fibrosarcomas. The patient with multicentric fibrosarcoma had numerous osteolytic osseous lesions and two soft tissue nodules at the pelvic girdle (Fig. 13.31).

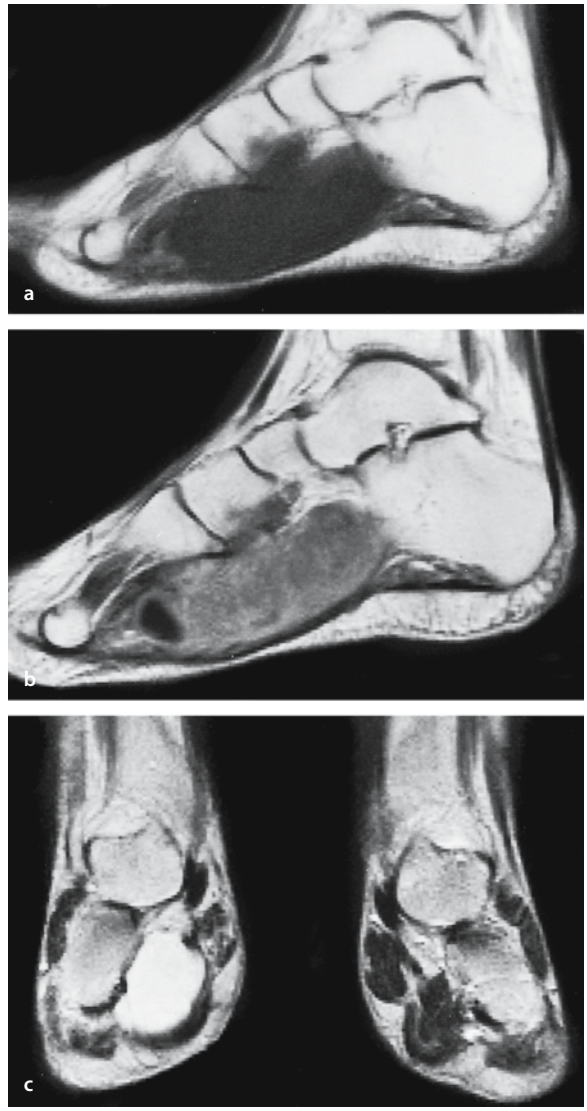

Fig. 13.30 a–c. Fibrosarcoma of the foot in a 34-year-old man. **a** Sagittal spin-echo T1-weighted MR image. **b** Sagittal spin-echo T1-weighted MR image after gadolinium contrast injection. **c** Coronal spin-echo T2-weighted MR image. A large fusiform-mass lesion is present at the foot deep to the plantar aponeurosis, with involvement of the medial cuneiform bone. Overall signal intensity on the T1-weighted image is low (**a**). The lesion shows moderate enhancement, with a nonenhancing (necrotic?) nodule at the distal part (**b**). On the T2-weighted image, the lesion is of homogeneous high signal intensity (**c**). Age, location, and MRI characteristics suggest a malignant tumor but do not allow further histological typing

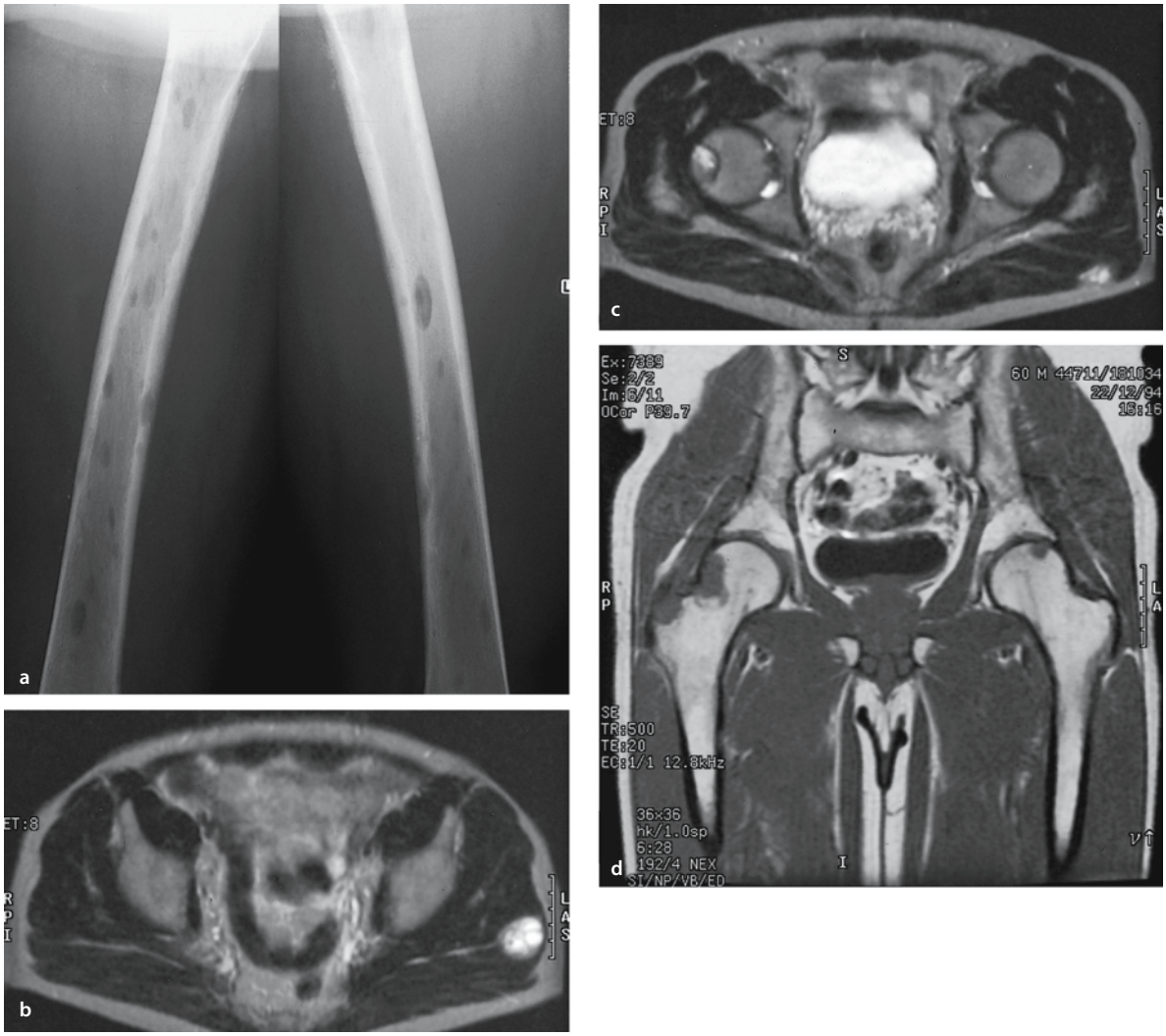

Fig. 13.31 a–d. Fibrosarcoma multiforme in a 50-year-old man. **a** Radiographs of both femoral shafts. **b** Axial spin-echo T2-weighted MR image at the level of the acetabulum. **c** Axial spin-echo T2-weighted MR image at the level of the femoral heads. **d** Coronal spin-echo T1-weighted MR image. On conventional radiographs there are multiple, oval, purely osteolytic lesions in cortical bone of both femora (**a**). On the T2-weighted image, there is a rounded lesion within the left gluteus maximus muscle, consisting of multiple lobules of high signal intensity, separated by septa of intermediate signal intensity (**b**). On the T2-weighted image at the level of the femoral heads, there is an inhomogeneous lesion within the right femoral head, partly of high signal intensity. There is a small, high-intensity soft tissue lesion in the gluteus maximus muscle on the left side (**c**). On the coronal view, there are multiple lesions of intermediate signal intensity at both femoral heads and right greater trochanter (**d**). Coexistence of bone and soft tissue lesions is a rare finding in fibrosarcoma. Differentiation from metastatic fibrosarcoma remains difficult even histologically

13.6.2 Myxofibrosarcoma

Myxofibrosarcoma (MFS), formerly known as myxoid malignant fibrous histiocytoma, is a malignant fibrous lesion that preferentially affects adults (mean age 66 years). It exhibits a slight male predominance. The majority of patients present with a slowly enlarging and painless mass. Most lesions (80%) arise in the extremities, and less frequently in the trunk, retroperitoneum, head and neck, pelvis, and penis. Seventy percent of the masses are located in the subcutis; they commonly have very infiltrative margins [59]. A MFS lesion is defined as low grade if 30% or more is of myxoid component, 20% or less is solid area and only focal, 10% or less is tumor necrosis [35]. Low-grade MFS occur more frequently in a superficial location [62].

Histopathologically, a nodular growth pattern is seen. The myxoid matrix contains elongated, curvilinear, thin-walled capillaries, and fusiform, round or stellate cells with slightly eosinophilic cytoplasm. Low-grade lesions have a hypocellular, mainly myxoid

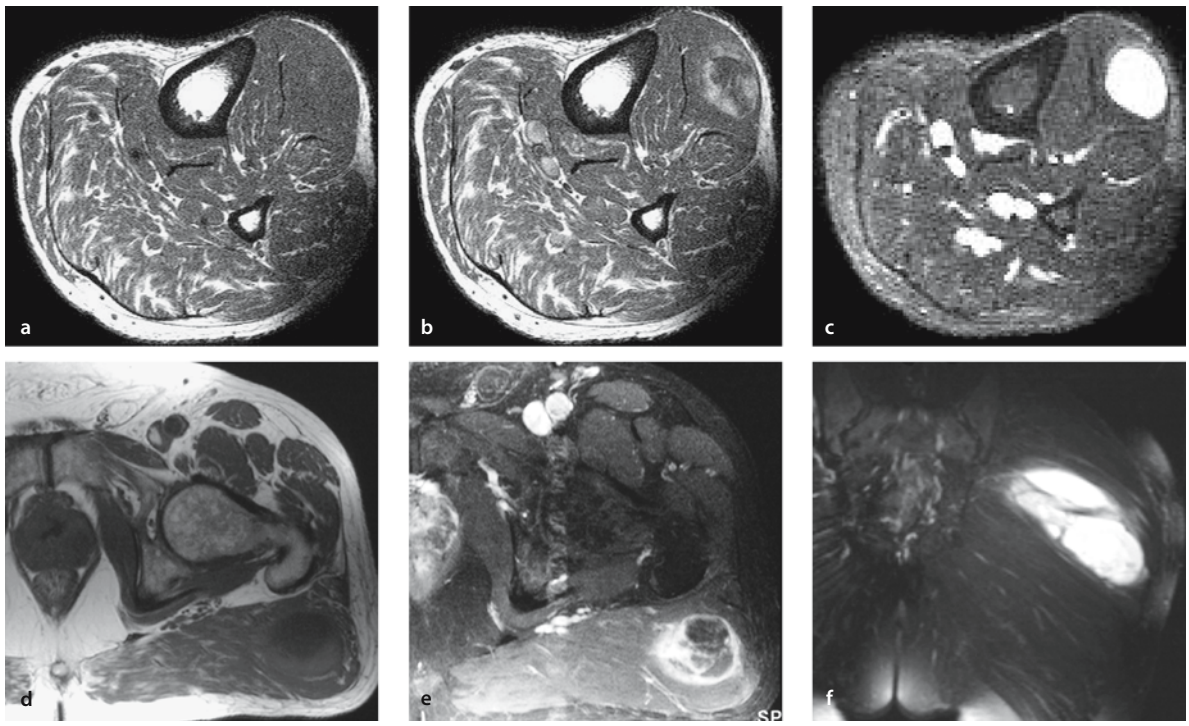

Fig. 13.32 a–f. Two cases of myxofibrosarcoma. **a** Axial spin-echo T1-weighted MR image. **b** Axial spin-echo T1-weighted MR image after gadolinium contrast injection. **c** Axial short-tau inversion recovery MR image. **d** Axial spin-echo T1-weighted MR image. **e** Axial spin-echo T1-weighted MR image after gadolinium contrast injection with fat suppression. **f** Coronal spin-echo T2-weighted MR image: a first one at the left lower leg (**a–c**), a second one at the left gluteal region (**d–f**). Both lesions are of low SI on T1-weighted MR images (**a, d**), show septal and peripheral enhancement after contrast administration (**b**, **e**) and are of very high SI on T2-weighted MR images (**c**, **f**) due to abundant myxoid components

aspect, whereas, in high-grade myxofibrosarcoma, high mitotic activity, pleomorphism, and intratumoral necrosis is seen [59].

Mentzel et al. describe local recurrences in 54% of their cases (follow-up of 5–300 months) and metastases in 17%. Neither the depth of the primary lesion nor the histological grade influences the incidence of local recurrence. However, because only intermediate- and high-grade neoplasms metastasize, it is important to recognize low-grade myxofibrosarcoma, because incorrect initial diagnosis and treatment may result in local recurrence, with progression to a higher-grade lesion that has the capability to metastasize [27, 59].

Imaging findings are sparsely reported. On ultrasound scans, a well-circumscribed hypoechoic mass is seen. On T1-weighted MR images, the lesion is homogeneous and has intermediate SI [70]. T2-weighted images reflect the myxoid content of low- and intermediate-grade myxofibrosarcoma, the myxoid content being inversely proportional to the cellularity and the grade of the tumor. High-grade myxofibrosarcoma is not easily distinguished from other adult pleomorphic sarcomas as well histopathologically as on imaging [39] (Fig. 13.32).

Low-grade myxofibrosarcoma may not be confused with low-malignancy fibromyxoid sarcoma, another myxoid mesenchymal sarcoma with fibroblastic differentiation, which has – in contrast to low-grade myxofibrosarcoma – an indolent but ultimately malignant clinical course [57, 58].

13.6.3 Fibromyxoid Sarcoma

Low-grade fibromyxoid sarcoma is a slow-growing, rare neoplasm that preferentially affects young and middle-aged adults (median age 45 years) (Fig. 13.33). Very occasionally it affects children. Most lesions arise from the deep soft tissues at the lower limb or thoracic wall, and less frequently the groin, buttock, axilla, and retroperitoneum [18]. The majority of cases occur in a subfascial location. They are often large at the time of diagnosis.

Histopathologically, the lesion is characterized by intermingled fibrous and myxoid areas, a whorled growth pattern, and bland fibroblastic spindle cells. Cellularity is low and mitotic figures are uncommon.

In contrast to low-grade myxofibrosarcoma, low-grade fibromyxoid sarcoma has an aggressive clinical

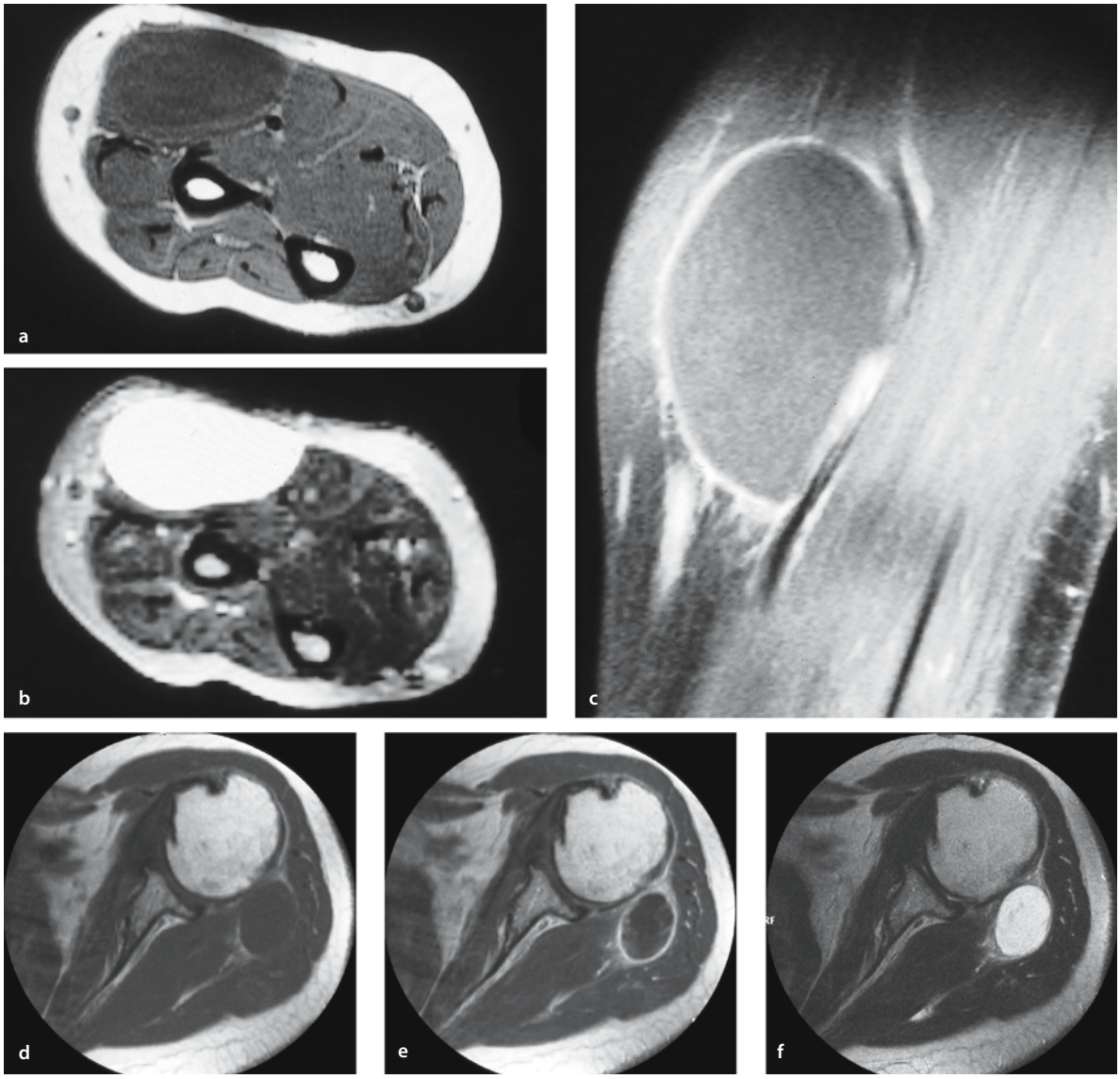

Fig. 13.33 a–f. Two cases of fibromyxoid sarcoma (**a–c**, **d–f**). **a** Axial spin-echo T1-weighted MR image. **b** Axial spin-echo T2-weighted MR image. **c** Sagittal spin-echo T1-weighted MR image after gadolinium contrast injection with fat suppression. **d** Axial spin-echo T1-weighted MR image. **e** Axial spin-echo T1-weighted MR image after gadolinium contrast injection. **f** Axial spin-echo T2-weighted MR image. Both have similar MRI features. Both lesions are of very low SI on T1-weighted MR image (**a, d**), of very high SI on T2-weighted MR image (**b**, **c**) and show only minimal capsular enhancement after contrast administration (**c**, **f**). MR findings reflect the high content of myxoid tissue of both tumors

course characterized by multiple recurrences and with the potential for metastasis to lungs and occasionally to bone. However, recent series show recurrences, metastases, and death from disease in only 9 %, 6 %, and 2 % of patients, respectively. [21, 31].

Imaging features of low-grade fibromyxoid sarcoma are sparsely reported. Koh has reported on two patients with intralesional nodules, one with a large, ovoid mass within the thigh, some of these nodules showing a target-like appearance. A second lesion was dumbbell-shaped with invasive features. There was no intralesional hemorrhage or necrosis.[43].Two high-grade fibromyxoid sarcomas in our series showed a pseudocystic appearance on MR images, i. e., low SI on T1-, high SI on T2-, and only faint, capsular enhancement on Gd contrast T1-weighted images.(Fig. 13.33).

13.7 Strategy

Because they frequently have a characteristic localization and age at presentation (childhood or midlife), tumors of fibrous tissue are diagnosed clinically and not by means of medical imaging. Clinical suspicion may be confirmed by ultrasound, which otherwise has only limited value in diagnostic workup except for demonstration or intratumoral calcifications. Conventional radiography or, even better, CT may confirm the presence of calcifications and show concomitant osseous involvement as a rare finding.

After a lesion has been detected clinically and/or on ultrasound, further evaluation by MRI is mandatory. MRI is able to demonstrate the exact localization, extent, and margins of the lesion. Intratumoral areas of low SI on T2-weighted images that do not enhance on T1-weighted images after Gd contrast administration represent fibrous components of mature tumors of fibrous tissue. Areas of high SI on T2-weighted images that enhance on T1-weighted images after Gd contrast administration represent nonfibrous components of immature tumors of fibrous tissue. Intratumoral necrosis is a rare finding even in fibrosarcoma.

MRI also shows the natural evolution of tumors of fibrous tissue, which have high SI in the initial stages and low SI on T2-weighted images in later stages, paralleling the histological evolution from hypercellular in the initial to more collagenous in the mature, later stage. Staging by MRI helps the physician to choose adequate therapy, leading to a decrease in tumor recurrence because of incomplete surgery.

The purposes of imaging of fibrous tumors in children described by Eich et al. [15] are:

1. Confirmation of a clinically suspected mass
2. Characterization of the mass with regard to location, extension, structure, and margins
3. Determination of either unifocal or multifocal disease, or metastases
4. Observation of additional features as part of a systemic disorder (e.g., Gardner syndrome, hyaline fibromatosis)
5. Formulation of a tentative diagnosis
6. Assistance for biopsy or excision
7. Follow-up for documentation of regression, progression, recurrence, or secondary spread.

Things to remember:

1. Tumors of connective tissue are common.
2. Histopathological and imaging features are related to age of the lesions.
3. Benign tumors mostly have a characteristic location (giant cell tumor of the tendon sheath, elastofibroma, palmar and plantar fibromatosis, nuchal fibroma, abdominal desmoid, etc.).
4. Desmoid tumors present with low-SI components also on T2-weighted MR images; they are aggressive lesions, which frequently recur after surgical resection.
5. Fibromatosis colli is seen within the sternocleidomastoid muscle in newborns.
6. Hemangiopericytoma moves from the vascular to the connective tissue tumors.
7. Myxofibrosarcoma replaces malignant fibrous histiocytoma in the new WHO classification.

References

1. Ablin DS, Jain K, Howell L, West DC (1998) Ultrasound and MR imaging of fibromatosis colli. Pediatr Radiol 28:230–233
2. Ackman J, Whitman G, Chew F (1994) Aggressive fibromatosis. Am J Roentgenol 163:544
3. Akisue T, Matsumoto K, Kizaki T, Fujita I, Yamamoto T, Yoshiya S, Kurosaka M (2003) Solitary fibrous tumor in the extremity: case report and review of the literature. Clin Orthop 411:236–244
4. Allen RA, Woolner LB, Ghormley RK (1995) Soft tissue tumors of the sole with special reference to plantar fibromatosis. J Bone Joint Surg 37:14–26
5. Casillas J, Sais G, Greve J, Iparraguirre M, Morillo G (1991) Imaging of intra- and extraabdominal desmoid tumors. Radiographics 11:959–968
6. Chateil JF, Brun M, Lebail B, Perel Y, Casteu JF, Diard F (1995) Infantile myofibromatosis. Skeletal Radiol 24:629–632
7. Cintora E, Del Cura J, Ruiz J, Grau M, Ereno C (1993) Case report 807. Skeletal Radiol 22:533–535
8. Col JY, Vannier JP, Chabrolle JP, Brottier C (1995) Fibromatosis found during prenatal ultrasonography. J Gynecol Obstet Biol Reprod 24:52–60
9. Crawford S, Harnsberger H, Johnson L et al (1988) Fibromatosis colli of infancy: CT and sonographic findings. AJR Am J Roentgenol 151:1183–1184
10. De Schepper A, Degryse H (1990) Imaging findings in a patient with Pentazocine-induced myopathy. AJR Am J Roentgenol 154:343–344
11. De Schepper A, Degryse H, Ramon F, Van Marck (1992) Extraabdominal desmoid tumors. J Belge Radiol 75:91–98
12. Devaney D, Livesley P, Shaw D (1995) Elastofibroma dorsi: MRI diagnosis in a young girl. Pediatr Radiol 25:282–285
13. Dong P, Seeger L, Eckardt J, Mirra J (1994) Juxtacortical aggressive fibromatosis of the forearm. Skeletal Radiol 23:560–563
14. Duda S, Bittner R, Laniado M, Lobeck H, Langer M (1989) Bildgebende Diagnostik der agressiven Fibromatosen und MRT-pathologischen Korrelation. Fortschr Röntgenstr 151: 57–62

15. Eich GF, Hoeffel JC, Tschäppeler H, Gassner I, Nilli UV (1998) Fibrous tumors in children: imaging features of a heterogeneous group of disorders. Pediatr Radiol 28:500–509
16. Einstein D, Tagliabue J, Desai R (1991) Abdominal desmoids: CT findings in 25 patients. AJR Am J Roentgenol 157:275–279
17. Enzinger F, Weiss S (1995) Soft tissue tumors, 3rd edn. Mosby, St Louis, pp 165–292
18. Evans HL (1993) Low-grade fibromyxoid sarcoma. A report of 12 cases. Am J Surg pathol 17:595–600
19. Feld R, Burk L, Mc Cue P, Mitchell D, Lackman R, Rifkin M (1990) MRI of aggressive fibromatosis: frequent appearance of high signal intensity on T2-weighted images. Magn Reson Imaging 8:583–588
20. Fletcher DM, Krishnan Unni K, Mertens F (2002) World Health Organization classification of tumours. pathology and genetics of tumours of soft tissue and bone. IARC, Lyon, pp 47–106
21. Folpe AL, Lane KL, Pauli G, Weiss JT (2000) Low-grade fibromyxoid sarcoma and hyalizing spindle cell tumor with giant rosettes: a clinicopathological study of 73 cases supporting their identity and assessing the impact of high-grade areas. Am J Surg Pathol 24:1353–1360
22. Fornage B (1995) Musculoskeletal ultrasound. Churchill Livingstone, New York
23. Fox MG, Kransdorf MJ, Bancroft LW, Peterson JJ, Flemming DJ (2003) MR imaging of fibroma of the tendon sheath. AJR Am J Roentgenol 180:1449–1453
24. Francis R, Dorovini-Zis K, Glazer G, Lloyd R, Amendola M, Martel W (1986) The fibromatoses: CT-pathologic correlation. AJR Am J Roentgenol 147:1063–1066
25. Frei S, Lange S de, Fechner R (1991) Nodular fasciitis of the elbow. Skeletal Radiol 20:468–471
26. Fromowitz F, Hurst L, Nathan J, Badalamente M (1987) Infantile fibromatosis with extensive calcification. Am J Surg Pathol 11:66–75
27. Fukunaga M, Fukunaga N (1997) Low-grade myxofibrosarcoma: progression in recurrence. Pathol Int 47:161–165
28. Gallego M, Millan J, Gil-Martin R, Cespedes M, Pulpeiro R, Salamanca J (1987) Juvenile hyalin fibromatosis: radiographic and pathologic findings of a new case. J Med Imaging 1:251–257
29. Gartlan MG, Hoffman HT, Haller JR, Dolan KD (1993) Fibrosarcoma of the posterior neck. Ann Otol Rhinol Laryngol 102:820–822
30. Gielen JL, De Schepper AM, Vanhoenacker F, Parizel PM, Wang XL, Sciot R, Weyler J (2004) Accuracy of MRI in characterization of soft tissue tumors and tumor-like lesions. A prospective study in 548 patients. Eur Radiol 14(12):2320–2330
31. Goodlad JR, Mentzel R, Fletcher CD (1995) Low-grade fibromyxoid sarcoma: clinicopathological analysis of eleven new cases in support of a distinct entity. Histopathology 26: 229–237
32. Hartman TE, Berquist T, Fetsch JF (1992) MR imaging of extraabdominal desmoids: differentiation from other neoplasms. AJR Am J Roentgenol 158:581–585
33. Hawnaur J, Jenkins J, Isherwood (1990) Magnetic resonance imaging of musculoaponeurotic fibromatosis. Skeletal Radiol 19:509–514
34. Hayward PG, Orgill DP, Mulliken JB, Perez-Atayde AR (1995) Congenital fibrosarcoma masquerading as lymphatic malformation: report of two cases. J Pediatr Surg 30:84–88
35. Huang HY, Lal P, Qin J, Brennan MF, Antonescu CR (2004) Low-grade myxofibrosarcoma: a clinicopathologic analysis of 49 cases treated at a single institution with simultaneous assessment of the efficacy of 3-tier and 4-tier grading systems. Hum Pathol 35(5):612–621
36. Ichikawa T, Koyama A, Fujimoto H et al (1994) Abdominal wall desmoid mimicking intraabdominal mass: MR features. Magn Reson Imaging 12:541–544
37. Ishii N, Matsui K, Ichiyama S, Takahashi Y, Nakajima H (1989) A case of infantile digital fibromatosis showing spontaneous regression. Br J Dermatol 121:129–133
38. Jabra A, Taylor G (1993) MRI evaluation of superficial soft tissue lesions in children. Pediatr Radiol 23:425–428
39. Kilpatrick SE, Ward WG (1999) Myxofibrosarcoma of soft tissues: cytomorphologic analysis of a series. Diagn Cytopathol 20:6–9
40. Kim E, Kim C, Romero J, Chung W, Isiklar A (1995) Different biologic features of desmoid tumors demonstrated with MR Imaging, RNSA, scientific exhibition, Poster 278 SK, Chicago, 25 Nov–1 Dec
41. Kingston CA, Owens CM, Jeanes A, Malone M (2002) Imaging of desmoid fibromatosis in pediatric patients. AJR Am J Roentgenol 178:191–199
42. Koenigsberg RA, Faro S, Chen X, Marlowe F (1995) Nodular fasciitis as a vascular neck mass. AJNR Am J Neuroradiol 17:567–569
43. Koh SH, Choe HS, Lee IJ, Park HR, Bae SH (2004) Low-grade fibromyxoid sarcoma: ultrasound and magnetic resonance findings in two cases. Skeletal Radiol 8 [Epub ahead of print]
44. Koujok K, Ruiz RE, Hernandez RJ (2004) Myofibromatosis: imaging characteristics. Pediatr Radiol 19 [Epub ahead of print]
45. Kransdorf M, Murphey M (1997) Imaging of soft tissue tumors. Saunders, Philadelphia, pp 143–186
46. Kransdorf M, Jelinek J, Moser R, Utz J, Hudson T, Neal J, Berrey B (1990) Magnetic resonance appearance of fibromatosis. Skeletal Radiol 19:495–499
47. Kransdorf M, Meis J, Montgomery E (1992) Elastofibroma: MR and CT appearance with radiologic-pathologic correlation. AJR Am J Roentgenol 159:575–579
48. Lang P, Suh KJ, Grampp S, Steinbach L, Steiner E, Peterfy C, Tirman P, Schwickert H, Rosenau W, Genant HK (1995) CT and MRI in elastofibroma. A rare benign soft tissue tumor. Radiologe 35:611–615
49. Lee T, Wapner K, Hecht P (1993) Current concepts review: plantar fibromatosis. J Bone Joint Surg [Am] 75:1080–1084
50. Liessi G, Tregnaghi A, Barbazza R, Scapinello A, Muzzio P (1991) Elastofibroma: CT and MR findings. J Belge Radiol 74:37–39
51. Liu P, Thorner P (1992) MRI of fibromatosis: with pathologic correlation. Pediatr Radiol 22:587–589
52. Lourie JA, Lwin KY, Woods C (1992) Fibroma of tendon sheath eroding 3rd metatarsal bone. Skeletal Radiol 21:273–275
53. Loyer E, Shabb N, Mahon T, Eftekhari F (1992) Fibrous hamartoma of infancy: MR-pathologic correlation. J Comput Assist Tomogr 16:311–313
54. Marin ML, Perzin KH, Markowitz AM (1989) Elastofibroma dorsa: benign chest wall tumor. J Thorac Cardiovasc Sur 98: 234–238
55. Massengill A, Sundaram M, Kathol M, El-Khoury G, Buchwalter J, Wade T (1993) Elastofibroma dorsi: a radiological diagnosis. Skeletal Radiol 22:121–123
56. Meiss-Kindblom J, Enzinger F (1996) Color atlas of soft tissue tumors. Mosby-Wolfe, St Louis
57. Mentzel T, Katenkamp D, Fletcher CD (1996) Low malignancy myxofibrosarcoma versus low malignancy fibromyxoid sarcoma. Distinct entities with similar names but different clinical course. Pathologe 17:116–121
58. Mentzel T, Calonje E, Wadden C, Camplejohn RS, Beham A, Smith MA, Fletcher CD (1996) Myxofibrosarcoma. Clinicopathologic analysis of 75 cases with emphasis on the low-grade variant. Am J Surg Pathol 20:391–405
59. Meyer C, Kransdorf M, Jelinek J, Moser R (1991) MR and CT appearance of nodular fasciitis. J Comput Assist Tomogr 15:276–279
60. Michal M, Fetsch JF, Hes O, Miettinen M (1999) Nuchal-type fibroma: a clinicopathologic study of 52 cases. Cancer 85:156–163
61. Morrison W, Schweitzer M, Wapner K, Lackman R (1994) Plantar fibromatosis: a benign aggressive neoplasm with a characteristic appearance on MR images. Radiology 193:841–845
62. Oda Y, Takahira T, Kawaguchi K, Yamamoto H, Tamiya S, Matsuda S, Tanaka K, Iwamoto Y, Tsuneyoshi M (2004) Low-grade fibromyxoid sarcoma versus low-grade myxofibrosarcoma in the extremities and trunk. A comparison of clinicopathological and immunohistochemical features. Histopathology 45(1):29

63. Ogose A, Hotta T, Emura I, Higuchi T, Kusano N, Saito H (2000) Collagenous fibroma of the arm: a report of two cases. Skeletal Radiol 29:417–420
64. O'Keefe F, Kim E, Wallace S (1990) Magnetic resonance imaging in aggressive fibromatosis. Clin Radiol 42:170–173
65. Posner MC, Shiu MH, Newsome JL, Hajdu SI, Gaynoe JJ, Brennan MF (1989) The desmoid tumor. Not a benign disease. Arch Surg 124:191–196
66. Pretorius E, Hrubain R, Fishman E (1995) Recurrent fibromatosis in a patient with breast carcinoma. Invest Radiol 30:381–383
67. Pulitzer D, Martin P, Reed R (1989) Fibroma of tendon sheath. Am J Surg Pathol 13:472–479
68. Quinn S, Erickson S, Dee P, Walling A, Hackbarth D, Knudson G, Mosely H (1991) MR Imaging in fibromatosis: results in 26 patients with pathologic correlation. AJR Am J Roentgenol 156:539–542
69. Reed M, Gooding G, Kerley S, Himebaugh-Reed M, Griswold V (1991) Sonography of plantar fibromatosis. J Clin Ultrasound 19:578–582
70. Reuther G, Mutschler W (1988) An unusual location of a myxofibrosarcoma. ROFO Fortschr Geb Rontgenstr Nuklearmed 149:544–545
71. Robbin MR, Murphey MD, Temple HT, Kransdorf MJ, Choi JJ (2001) Imaging of musculoskeletal fibromatosis. Radiographics 21:585–600
72. Samadi DS, McLaughlin RB, Loevner LA, LiVolsi VA, Goldberg AN (2000) Nuchal fibroma: a clinicopathological review. Ann Otol Rhinol Laryngol 109:52–55
73. Shankwiler RA, Athey PA, Lamki N (1989) Aggressive infantile fibromatosis. Clin Imaging 13:127–129
74. Shields CJ, Winter DC, Kirwan WO, Redmond HP (2001) Desmoid tumors. Eur Journal Surg Oncol 27(8):701–706
75. Shimizu S, Hashimoto H, Enjoji M (1984) Nodular fasciitis: an analysis of 250 patients. Pathology 16:161–166
76. Sifumba S, Thomson SR, Madaree R (1993) Desmoids don't die. S Afr Med J 83:536–537
77. Sundaram M, Duffrin H, McGuire MH, Vas W (1988) Synchronous multicentric desmoid tumors (aggressive fibromatosis) of the extremities. Skeletal Radiol 17:16–19
78. Tourne Y, Saragaglia D, Butel J (1991) Les fibromes desmoïdes des parties molles à localisation extraabdominale. Ann Radiol 34:267–272
79. Tung G, Davis L (1993) The role of magnetic resonance imaging in the evaluation of the soft tissue mass. Crit Rev Diagn Imaging 34:239–308
80. Vandevenne JE, De Schepper AM, De Beuckeleer L, Van Marck E, Aparisi F, Bloem JL, Erkorkmaz Z, Brijs S (1997) New concepts in understanding evolution of desmoid tumors: MR imaging of 30 lesions. Eur Radiol 7:1013–1019
81. Vinnicombe S, Hall C (1994) Infantile fibrosarcoma: radiological and clinical features. Skeletal Radiol 23:337–341
82. Wagstaff MJD, Raurell A, Perks AGB (2004) Multicentric extraabdominal desmoid tumors. Br J Plast Surg 57 (4):362–365
83. Wang X, De Schepper A, Vanhoenacker F, De Raeve H, Gielen J, Aparisi F, Rausin L, Somville J (2002) Nodular fasciitis: correlation of MRI findings and histopathology. Skeletal Radiol 31:155–161
84. Wassenaar W (1994) Infantile myofibromatosis. Rad Doc 94–10
85. Wetzel L, Levine E (1990) Soft tissue tumors of the foot: value of MR imaging for specific diagnosis. AJR Am J Roentgenol 155:1025–1030
86. Wuisman P, Roessner A, Blasius S, Edel G, Vestring R, Winkelmann W (1994) Solitary congenital or infantile (desmoid-type) fibromatosis of the proximal end of the tibia. Skeletal Radiol 23:381–384
87. Yacoe M, Bergman G, Ladd A, Hellman B (1993) Dupuytren's contracture: MR imaging findings and correlation between MR signal intensity and cellularity of the lesions. AJR Am J Roentgenol 160:813–817
88. Yao L, Toranji S, Doberneck S, Eckardt J (1994) Case report 818. Skeletal Radiol 23:217–219